

**Dissertation**

**Intramedullary application of novel  
bioresorbable implants in the growing rat  
for osteosynthesis**

submitted by

**Mag.rer.nat. Elisabeth MARTINELLI**

for the Academic Degree of

**Doctor of Medical Science**

at the

**Medical University of Graz**

Department of Pediatric and Adolescent Surgery

Department of Orthopaedics and orthopaedic Surgery

under the Supervision of

**Assoc.Prof.PD.Dr.med. Annelie-Martina**

**WEINBERG**

**2015**

## Eidesstattliche Erklärung

*Ich erkläre ehrenwörtlich, dass ich die vorliegende Arbeit selbständig angefertigt und abgefasst und jene Personen und Institutionen, die am Zustandekommen der Forschungsdaten beteiligt waren, namentlich genannt habe. Andere als die angegebenen Quellen habe ich nicht verwendet und die den benutzten Quellen wörtlich oder inhaltlich entnommenen Stellen habe ich als solche kenntlich gemacht. Die Arbeit an der Dissertation und daraus entstandener Publikationen wurde gemäß den Regeln der "Good Scientific Practice" durchgeführt.*

## Declaration

*I hereby declare that this thesis is my own original work and that I have fully acknowledged by name all of those individuals and organisations that have contributed to the research for this thesis. Due acknowledgement has been made in the text to all other material used. Throughout this thesis and in all related publications I followed the guidelines of "Good Scientific Practice".*

30.09.2015,

---

Date,

ELISABETH MARTINELLI

---

(Signature)

# Danksagung

Bei der Arbeit an einer Dissertation sind über die Jahre eine Vielzahl an Personen beteiligt, die mit einem unterschiedlich lange Wegstrecken bestreiten:

Mein vorrangiger Dank gilt meiner Familie, das Wichtigste für mich auf der Welt.

Ich hatte das Glück in meinen Arbeitskollegen eine weitere Familie gefunden zu haben. Nicht nur Kollegen sondern auch Freunde sind Johannes Eichler, Anastasia Myrissa, Rebecca Ruedl, Vera Fengler, die nicht nur für mein leibliches sondern oft auch für mein geistiges Wohl gesorgt haben!

Aber besonderer Dank gilt Annelie-Martina Weinberg, die mit Energie und Stärke immer voran gegangen ist und Peter Uggowitzer, der oft auch Mentor in nicht wissenschaftlichen Fragen war.

Unzählige Freunde, die mich in dieser Zeit angefeuert, bestärkt, beschützt, getragen, belohnt aber auch geschimpft, korrigiert oder ignoriert und Prioritäten gesetzt haben, wenn es gerade nötig war. Ihr wart mir Muse, Inspiration, Ablenkung, Konzentration und Lebensfreude!! Es weiß schon jeder, wer gemeint ist...

Man möge mir die Länge verzeihen, aber ich bin privilegiert so außergewöhnliche Menschen kennen gelernt zu haben!

# Table of Contents

<b>List of Figures</b>	<b>VII</b>
<b>List of Tables</b>	<b>X</b>
<b>1 Introduction</b>	<b>1</b>
1.1 Paediatric injuries . . . . .	1
1.2 Fracture healing in children . . . . .	3
1.3 Osteosynthesis of long bone fractures in children . . . . .	7
1.3.1 Conservative treatment . . . . .	10
1.3.2 Surgical treatment . . . . .	10
1.4 Bioresorbable materials . . . . .	12
1.4.1 Requirements bioresorbable materials in children . . . . .	13
1.5 Aims of this thesis . . . . .	15
1.5.1 Aim 1) In vivo degradation of novel bioresorbable composites in the femur of rats . . . . .	15
1.5.2 Aim 2) Biocompatibility and osteoinductive properties of PHB bone implants . . . . .	16
1.5.3 Aim 3) Immunological response to bone injuries and implan- tation of a biodegradable polymer . . . . .	16
<b>2 Materials and Methods</b>	<b>18</b>

2.1	Implants . . . . .	18
2.2	Experimental design . . . . .	20
2.3	Ethical approval . . . . .	23
2.4	Surgical procedure . . . . .	23
2.5	Blood sampling . . . . .	26
2.6	Phagocytic assay . . . . .	27
2.7	Flow cytometric analysis . . . . .	27
2.8	Euthanasia . . . . .	28
2.9	Microfocus computed tomography <i>in vivo</i> . . . . .	28
2.10	Microfocus computed tomography <i>ex vivo</i> high resolution . . . . .	30
2.11	Push out tests . . . . .	31
2.12	Histological sample processing . . . . .	32
2.13	Statistics . . . . .	34
<b>3</b>	<b>Results</b>	<b>35</b>
3.1	Aim 1) <i>In vivo</i> degradation of novel bioresorbable composites in the femur of rats . . . . .	37
3.1.1	Microfocus computed tomography <i>in vivo</i> . . . . .	37
3.1.2	Microfocus computed tomography high resolution <i>ex vivo</i> . . . . .	42
3.2	Aim 2) Biocompatibility and osteoinductive properties of PHB bone implants . . . . .	46
3.2.1	Microfocus computed tomography <i>in vivo</i> . . . . .	46
3.2.2	Push out tests . . . . .	48
3.2.3	Histological evaluation . . . . .	51
3.3	Aim 3) Immunological response to bone injuries and implantation of a biodegradable polymer . . . . .	57
3.3.1	Phagocytic assay . . . . .	57
3.3.2	Microfocus computed tomography <i>in vivo</i> . . . . .	60

<b>4 Discussion</b>	<b>63</b>
4.1 Aim 1) In vivo degradation of novel bioresorbable composites in the femur of rats . . . . .	63
4.2 Aim 2) Biocompatibility and osteoinductive properties of PHB bone implants . . . . .	65
4.3 Aim 3) Immunological response to bone injuries and implantation of a biodegradable polymer . . . . .	67
<b>5 Conclusion</b>	<b>70</b>
<b>References</b>	<b>72</b>

# Abbreviations

BV	Bone Volume
CDC	Centers for Disease Control
DNA	Deoxyribonucleic acid
EU	European Union
ESIN	Elastic stable intramedullary nailing
FSC	Forward scatter
FDA	The Food and Drug Administration
FITC	Fluorescein isothiocyanate
HU	Hounsfield units
IL	Interleukine
M	Mean
$\mu$ CT or micro CT	Microfocus computed tomography
N	Number
P	Polyhydroxybutyrate
P3Z	Polyhydroxybutyrate with 3w% Zircondioxid
P3Z30H	Polyhydroxybutyrate with 3w% Zircondioxid and 30w% Herafill <sup>®</sup>

P30H	Polyhydroxybutyrate with 30w% Herafill®
P40Mg	Polyhydroxybutyrate with 40w% Magnesium powder
PHA	Polyhydroxyalkanoate
PHB	Polyhydroxybutyrate
PLA	Poly(lactic acid)
PLGA	Poly(lactic-co-glycolic acid)
PLLA	Poly (L-lactic acid)
PG	Prostaglandine
R	Range
SD	Standard deviation
SG	Surface gain
SSC	Side scatter
TGF	Transforming growth factor
TNF	Tumor necrosis factor
US	United States
TV	Total volume
VG	Volume gain
WHO	World Health Organisation

# List of Figures

1.1	a) Torus or buckling fracture b) Greenstick fracture c) Bow fracture [1]	5
1.2	Type I - V Salter-Harris classification [2]	6
1.3	Example of callus formation [1]	8
1.4	Examples of a) Wire osteosynthesis, b) Screw fixation, c) Tension band wiring, d) Plate osteosynthesis and e) ESIN fixation [2]	11
2.1	native PHB Implant	20
2.2	Bilateral transcortical implantation of pins of different PHB composites	22
2.3	Surgical procedure of transcortical implantation in the femur of rats (friendly courtesy of Dr.med.univ. K. Angerpointner) [3]	25
2.4	Blood sampling through tongue veins	26
2.5	After 6 months of implantation, PHB with 30w% Herafill <sup>®</sup> calculation of BV/TV with MIMICS <sup>®</sup>	30
2.6	Push out tests: a) Optical assessment of the implant b,c) Experimental setup for mechanical pin displacement	32
2.7	Histological slice of PHB with Zircondioxide and Herafill <sup>®</sup> after 6 months. The red arrows indicate bone adherence.	33
3.1	3D reconstruction of bone with native PHB implant, unseen because of similar density like environmental tissue	35

3.2	native PHB implanted into the femur of rats, only new formed bone around the implant is visible in 2D reconstruction . . . . .	36
3.3	PHB with 3w% Zircondioxid at different time points of implantation: month 1 (a) sagittal 2D, (e) and 3D reconstruction; month 3 (b) sagittal 2D, (f) and 3D reconstruction; month 6 (c) sagittal 2D, (g) and 3D reconstruction; and month 9 (d) sagittal 2D, (h) and 3D reconstruction . . . . .	38
3.4	PHB with 3w% Zircondioxid and 30w% Herafill <sup>®</sup> at different time points of implantation: month 1 (a) sagittal 2D, (e) and 3D reconstruction; month 3 (b) sagittal 2D, (f) and 3D reconstruction; month 6 (c) sagittal 2D, (g) and 3D reconstruction; and month 9 (d) sagittal 2D, (h) and 3D reconstruction . . . . .	39
3.5	PHB with 30w% Herafill <sup>®</sup> at different time points of implantation: month 1 (a) sagittal 2D, (d) and 3D reconstruction; month 3 (b) sagittal 2D, (e) and 3D reconstruction; and month 6 (c) sagittal 2D, (f) and 3D reconstruction . . . . .	40
3.6	PHB with 40w% Magnesium powder at different time points of implantation: month 1 (a) sagittal 2D, (e) and 3D reconstruction; month 3 (b) sagittal 2D, (f) and 3D reconstruction; month 6 (c) sagittal 2D, (g) and 3D reconstruction; and month 9 (d) sagittal 2D, (h) and 3D reconstruction . . . . .	41
3.7	In Mimics <sup>®</sup> segmented and calculated volume and surface of P3Z30H implant after 6 months . . . . .	42
3.8	High resolution scan of explanted P3Z30H implant after 9 months. . .	43
3.9	High resolution scan of explanted P40Mg implant after 9 months with measured diameter and length of implant . . . . .	44
3.10	3D bone formation calculated and segmented in Mimics <sup>®</sup> of native PHB after 6 months . . . . .	46

3.11 3D bone formation calculated and segmented in Mimics <sup>®</sup> of PHB with Zircondioxide after 6 months . . . . .	46
3.12 3D bone formation calculated and segmented in Mimics <sup>®</sup> of PHB with Zircondioxide and Herafill <sup>®</sup> after 6 months . . . . .	47
3.13 Explants after 1 month of implantation; left PHB with 30w% Herafill <sup>®</sup> , right PHB with 40w% Mg . . . . .	49
3.14 Push out results of PHB composites - the pin was displaced by press- ing a cylindrical steel rod with constant velocity against it [4]. . . . .	50
3.15 Share energy results of PHB composites - calculated by dividing the force maximum (point of failure) by the area of the implant bone interface [4]. . . . .	51
3.16 Histological slice of native PHB after 1, 3 and 6 months. . . . .	53
3.17 Histological slice of PHB with Zircondioxide after 1, 3 and 6 months. . . . .	54
3.18 Histological slice of PHB with Zircondioxide and Herafill <sup>®</sup> after 1, 3 and 6 months. . . . .	55
3.19 Results of mean bone adherence measurements on histological slices . . . . .	56
3.20 Phagocyte level during 8 weeks of observation in the control (C), Sham (S) and experimental group with PHB implant (B) . . . . .	58
3.21 Sham group 1 week, 4 weeks and 8 weeks after surgery . . . . .	61
3.22 Experimental group 1 week, 4weeks and 8 weeks after surgery . . . . .	62

# List of Tables

2.1	PHB composite materials used in this study. . . . .	18
2.2	Biomechanical properties of PHB composites [4] compared to biomechanical properties of PGA, PLLA and PLGA screws [5] . . . . .	19
2.3	Experimental procedure divided in five groups: P = native PHB, P3Z = PHB with 3w% Zircondioxid, P3Z30H = PHB with 3w% Zircondioxid and 30w% Herafill <sup>®</sup> , P30H = PHB with 30w% Herafill <sup>®</sup> and P40M = PHB with 40w% Magnesium powder . . . . .	21
2.4	Experimental procedure in groups: B = Experimental group with PHB, S = Sham group, C = Control group . . . . .	23
3.1	Measured implant volume and surface with mean values (M), measurement range (R) and standard deviation (SD) after 3, 6 and 9 months <i>in vivo</i> . Original implant volume and surface were calculated from a cylindric shape of 1.6 mm in diameter and a hight of 8 mm [6].	45
3.2	Measured percentage of volume gain (VG) and surface gain (SG) after 3, 6 and 9 months [6]. . . . .	45
3.3	Calculated bone volume (BV) to total volume (TV) fraction around the implant. $N \geq 6$ samples were used for all PHB composites at each timepoint [6]. . . . .	48

# Abstract

**Introduction** In the development of biodegradable implants for children several special features have to be addressed: Fracture healing in children is faster and the bone takes over weight-bearing earlier than adults permitting fast degradation of the implant material. So biodegradable implants would be of substantial benefit in paediatric patients. But due to the special conditions of the children's bone, several steps regarding materials, biomechanics, the degradation in the bone and the bony answer have to be considered.

**Materials & Methods** Cylindrical pins made of *Poly(3-hydroxybutyrate)* (PHB) with different additives were analysed: pure PHB, PHB with 3w% Zircondioxid, PHB with 3w% Zircondioxid and 30w% Herafill<sup>®</sup>, an alternative bone material, PHB only with 30w% Herafill<sup>®</sup> and PHB with 40w% Magnesium powder. Two identical pins were implanted in the femoral bones of growing Spraque Dawley<sup>®</sup> rats. Continuous micro computed tomography scans were performed to asses the degradation performance and new bone adherence after 1, 3, 6 and 9 months of implantation of the composite materials. Additionally, push out tests, histological slides and high resolution scans *ex vivo* were made to compare bone reaction. Blood examinations evaluated the response of the innate immune system during the study period.

**Results** Added Magnesium powder was degrading faster and dissolved of the PHB network, but remaining PHB showed no enhanced degradation process. The whole implant was too brittle for proper handling during the implantation process and the push out tests after 1 month showed the lowest forces of all tested PHB implants. Also the additives Zircon dioxide and Herafill<sup>®</sup> could not accelerate the degradation process. Again with new additives, the resolution between implant and surface was not high enough to get valid volume and surface values with  $\mu$ CT scans. But it was possible to compare bone reactions and new bone formations within the different PHB groups. The high tolerance of tissue and bone to the implant in histological slices is promising. Over the time and the healing process, the bone fused with the implant and no inflammatory or adverse tissue reaction was observed.

Compared to Sham group with bone injury and trauma, the implant material shows no further immune reactions. The negative immunological effects of anaesthesia and surgery are seen in the first week after surgery in the sham and experimental group. After 4 weeks, the drill hole is healed and the bone remodelling started. This study confirms that PHB as a bioresorbable implant does not provide any significant further adverse effects compared to the Sham group, a good bone adherence and new bone formation can be observed in the  $\mu$ CT pictures.

**Discussion** Although PHB is a natural material produced by bacteria, the use as an implant for children in its native composition seems to be inappropriate due to its long degradation process. Because of the low degradation rate at the one side and the good tissue and bone tolerance on the other side, other fields of application should be considered. Coatings of permanent implants should be mentioned and it is also an alternative to PLA which is used for sutures, stents, dialysis, scaffolds and drug delivery devices.

# Zusammenfassung

**Einleitung** Mehrere Aspekte sind in der Entwicklung von biodegradierbaren Implantaten für Kinder von Bedeutung: Die Frakturheilung ist schneller und der Knochen übernimmt rascher als bei Erwachsenen wieder Lasten, was eine kürzere Degradation des Materials erlaubt. Damit wären biodegradierbare Implantate von substanziellem Nutzen für pädiatrische Patienten. Wegen der besonderen Voraussetzungen im kindlichen Knochen sollten die Materialien, Biomechanik, Degradation im Knochen und die Knochenantwort genauer untersucht werden.

**Material & Methoden** Zylindrische Pins aus *Poly(3-hydroxybutyrate)* (PHB) mit unterschiedlichen Additiven wurden analysiert: pures PHB, PHB mit 3w% Zirkondioxid, PHB mit 3w% Zirkondioxid und 30w% Herafill<sup>®</sup>, ein alternatives Knochenersatzmaterial, PHB nur mit 30w% Herafill<sup>®</sup> und PHB mit 40w% Magnesium Pulver. Zwei identische Pins wurden in den Femur von wachsenden Sprague Dawley<sup>®</sup> Ratten implantiert. Nach 1, 3, 6 und 9 Monaten wurden microCT Scans durchgeführt, um das Degradationsverhalten der Komposite und den Knochenanwuchs zu beurteilen. Push Out Tests, histologische Schnitte und hoch auflösende Scans *ex vivo* wurden gemacht, um die Knochenreaktion auf die einzelnen Materialien zu vergleichen. Blutuntersuchungen während der Studie evaluierten die Antwort des angeborenen Immunsystem.

**Resultate** Das zugemischte Magnesium Pulver degradiert schneller und löst sich aus dem PHB Netzwerk heraus, das verbleibende PHB zeigt jedoch keinen beschleunigten Degradationsprozess. Das Implantat wird zu brüchig, um eine korrekte Handhabung während der Implantation zu gewährleisten. 1 Monat nach Implantation zeigt es die geringsten Push Out Energien im Vergleich zu den anderen PHB Kompositen. Auch Zirkondioxid und Herafill<sup>®</sup> konnten den Degradationsprozess nicht beschleunigen. Weiters verbessern diese Additive die Auflösung zwischen Implantat und Oberfläche nicht so weit, dass reproduzierbare, valide Werte für die Oberfläche und das Volumen des Implantats mit dem  $\mu$ CT berechnet werden konnten. Aber es war möglich Knochenreaktionen und Knochenneuf ormation in unterschiedlichen PHB Gruppen zu vergleichen. Die histologische Schnitte zeigen eine vielversprechende Gewebe- und Knochentoleranz auf das Implantates. Während des Heilungsprozesses wächst der Knochen gut an das Implantat an und weder Inflammation noch Gewebsveränderungen konnten festgestellt werden.

Verglichen zur Sham Gruppe in der ein Trauma gesetzt wurde, zeigt das Implantatmaterial keine zusätzlichen Reaktionen des Immunsystems. Eine Woche nach Operation zeigt sich ein immunologischer Effekt, der Anästhesie und Operation zugeordnet werden konnte. Nach 4 Wochen ist das Bohrloch verheilt und der Knochenumbau hat begonnen. Diese Studie zeigt, dass PHB als bioresorbierbares Implantat keine zusätzlichen signifikanten negativen Effekte hervorruft. Weiters konnte eine gute Knochenanlagerung in den  $\mu$ CT Bildern nachgewiesen werden.

**Diskussion** Obwohl PHB von Bakterien produziert wird, ist es als Implantat für Kinder in seiner nativen Form wegen der langen Degradationszeit ungeeignet. Trotzdem sollten wegen der hohen Gewebe- und Knochenverträglichkeit andere Anwendungsbereiche in Betracht gezogen werden. Es könnte als Coating von permanenten Implantaten angedacht werden oder als Alternative zu PLA, welches als Nahtmaterial, Stents, Gerüstmatrix und als Medikamentenretard Systeme genutzt wird.

# 1 Introduction

## 1.1 Paediatric injuries

Injuries are the number one cause of death in children all over the world. Accounting for 32% of all deaths of children between 1 and 14 years of age and even rising up to 64% in adolescents between 15 and 24 years of age in the European Union, injuries and their disabling consequences have a tremendous impact on health in this age groups. The European Union (EU) reports more than 5.000 deaths per year in children between 0 and 14 years of age [7], the U.S. Centers for Disease Control and Prevention (CDC) records more than 12.000 deaths in children between 0 and 19 [8] and the World Health Organisation (WHO) refers even about

*„...hundreds of thousands of children die each year from injuries or violence...“* [9].

Therefore, it is reliable that childhood injury is classified from all responsible authorities as a major public health problem across the world.

Under the age of 15 years, 7.8 million children have to be treated for an injury in European hospitals each year representing 19% of all hospital treated injuries although this age group accounts only 16% of the total population. This means that one out of 10 children incurring an injury requires emergency medical attention

and 11% of these children have to be admitted to hospital depending on the severity of the injury. About 70% of all causes of death and fatal injuries in children up to 14 years are incidences like road traffic accidents, falls from height and other falls, interpersonal violence and others. Additionally to these numbers, boys are at higher risk of incurring a fatal injury than girls and from the moment of birth up to adolescence, the risk for boys to sustain an injury almost doubles compared to that of girls. This higher risk strongly depends on the mechanism and place of occurrence of the accident and the activity of the victim. About 63% of the unintentional fatal injuries happen at home, in leisure time or during sports. Concerning these facts, it is not unexpected that upper and lower extremities are more often injured (up to 70%) than any other body part. The most frequent consequences of severe injuries are bruises and contusions (31%), open wounds (21%) and fractures (20%) [7] which are of special importance within a growing skeleton.

Although many reports in the last years focus on the causes of injuries and the sources how injury data is collected [7, 8, 9, 10], it is estimated that

*„...existing sources of data often underestimate the extend of injuries.“ [7]*

Police and ambulance reports, hospital inpatient registers, emergency department injury records and national insurance schemes provide only a very incomplete picture of the injury problem because they are not reported to the police or not registered elsewhere in the statistics. Additionally, the age range for what constitutes childhood is not universally agreed, it varies considerably cross cultures. The EU uses the term for the age up to 14 years and „*adolescents*“ between 15 and 24 years of age [7] compared to the WHO which tries to focus on „*children under the age of 18 years*“ [9].

## 1.2 Fracture healing in children

An injury is according to Baker defined as “... *the physical damage that results when a human body is suddenly subjected to energy in amounts that exceed the threshold of physiological tolerance – or else the result of a lack of one or more vital elements, such as oxygen...*” [11].

This energy, exceeding the threshold of physical tolerance, can result in bone fractures or even soft tissue injuries. In paediatric bone, the energy needed to incur a fracture is lower compared to adults due to a weaker cortical bone in children. Although most of the paediatric fractures are comparable with adults [2], there are some specifics to consider in a growing skeleton:

- The periosteum in paediatric bone is thicker than in adults and has also a higher osteogenic potential, which results in a better and faster fracture healing.
- The remodelling process of paediatric bone is faster than in adults. Remodelling is defined as reorganisation of fractured bone to correct orientation and shape. In children, increased growth in length is specific due to remodelling in long bones after injury [12].
- Depending on age and maturity, open growth plates (physis) are the weakest cartilage-like parts of the bone and often injured by fractures. The growing potential of the bone has to be taken in account to minimise the influence on the growth plate during therapeutic treatment.

The growing skeleton has a high potential to correct a malposition of a fractured bone. But the localisation within the skeleton and therefore the distance to the growth plate is of importance to classify the fracture for further treatment [2]. Therefore, the following complete and incomplete fracture types are frequent in children

and specific for injuries at immature bones:

### **Incomplete fractures**

At the growing skeleton, typical incomplete fractures are caused by bending and are usually located at the forearm. As so-called bending fractures, they include more or less always a wrong axis orientation of the bone. There are three different classifications of fractures depending on the age of the children:

- Classical greenstick fracture

Characteristically, as a transverse fracture only one half of the cortex is completely broken extending into the midportion of the bone without disrupting the other part of the cortex (see figure 1.1 b).

- Torus or buckling fracture

Caused by impaction, it is a result of too high forces along the longitudinal axis of the bone. Mainly the distal radial metaphysis is involved as a typical consequence of a fall. The latin word *torus* means swelling or protuberance (see figure 1.1 a).

- Bow fracture

The bone is deformed in a bending curve without any visible fracture line (see figure 1.1 c).

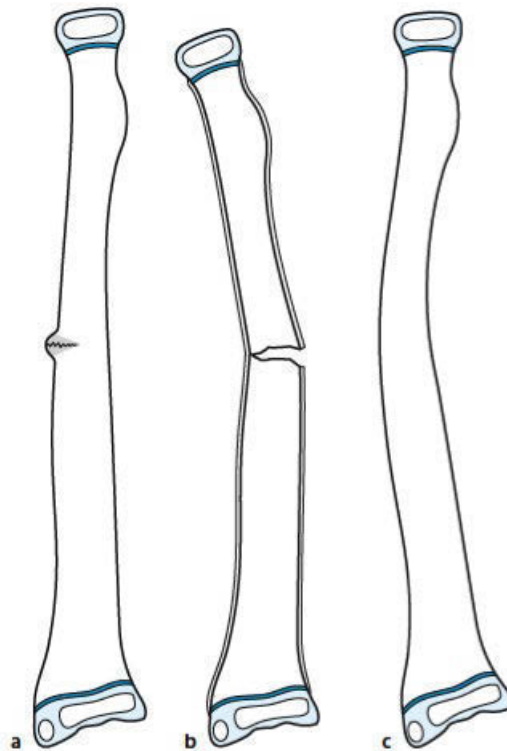


Figure 1.1: a) Torus or buckling fracture b) Greenstick fracture c) Bow fracture [1]

### Complete fractures

In physal fractures the physis (the so-called growth plate or epiphyseal plate, not present in adults) is involved occurring as common injury in 15% of childhood long bone fractures. There are various ways to classify fractures and more systematic classifications are currently in place [13]. Historically named after the medical doctor who described the fracture conditions first, paediatric fractures influencing the growth plate are specified by Robert B. Salter and W. Robert Harris in 1963 in the Salter-Harris classification [14]:

- Type I – Transverse fracture only within the growth plate resulting in displacement, metaphysis and epiphysis are not affected (see figure 1.2 a)

- Type II – Fracture through the growth plate and the metaphysis, no affected epiphysis (see figure 1.2 b)
- Type III – Fracture partially through the growth plate resulting in the epiphysis, no affected metaphysis (see figure 1.2 c)
- Type IV – Fracture affecting all parts of the bone, the growth plate, metaphysis and epiphysis (see figure 1.2 d)
- Type V – No displacement, but compression fracture of the growth plate (resulting in a decreased space between the epiphysis and metaphysis on x-ray) (see figure 1.2 e) [2, 15]

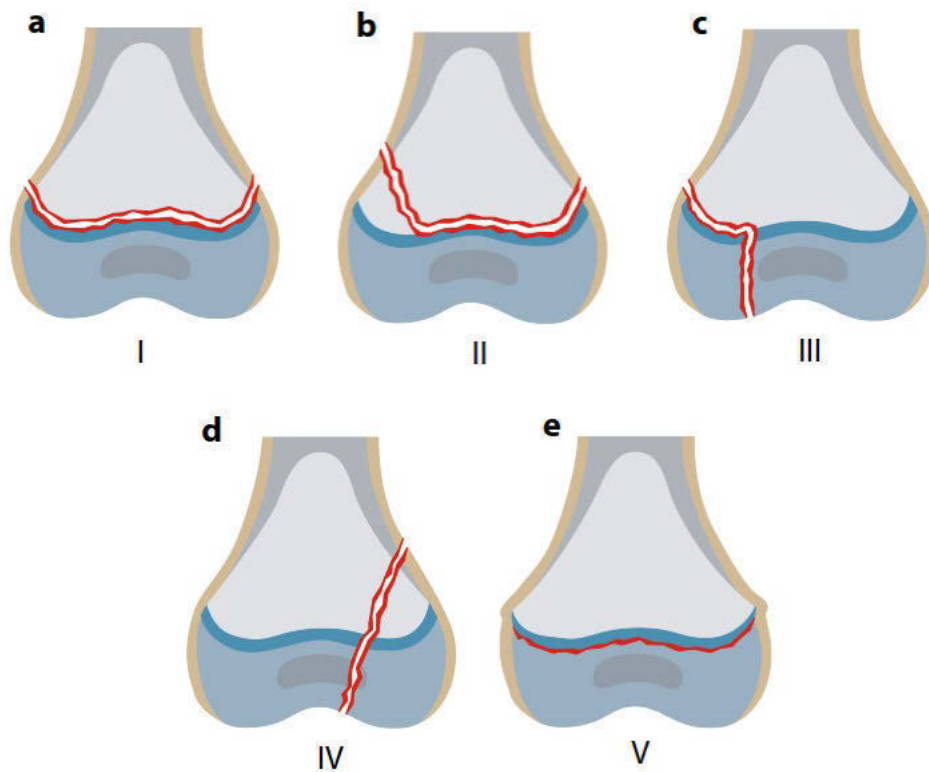


Figure 1.2: Type I - V Salter-Harris classification [2]

After radiological diagnostic, the classification of the type of fracture determines the kind of treatment [2, 15].

- Complete diaphyseal fractures have compared to the classical greenstick fracture both cortexes broken and are also quite common in children. But these kind of fractures are also frequently present in adults.

The final result of healing and remodelling of the bone mainly depends on the location of the fracture, proximity to the joint, three-dimensional orientation of the fragments and skeletal age [16]. All of these reasons have to be taken into account to prevent complications when paediatric fractures necessarily indicate surgical treatment.

### 1.3 Osteosynthesis of long bone fractures in children

Fracture healing in a growing skeleton is described in three phases: (i) the inflammatory phase is a reaction to the fracture associated haematoma. A collagenous net is built as basic structure and essential proteins for the new bone formation are produced; (ii) during the reparative phase lasting several weeks, mechanically inferior callus is formed which bridges the gap in the fractured bone (see figure 1.3); (iii) the remodelling phase can last months or even years replacing the callus by fully adequate bone [16].

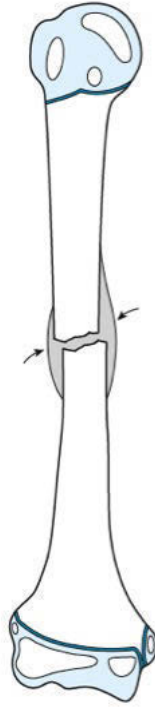


Figure 1.3: Example of callus formation [1]

The ongoing growth of bone describes the main issue in paediatric fracture fixation. At present, adapted metallic implants for adults are downscaled for children and used as osteosynthesis material, although children must not be understood as “small adults”. Paediatric implants and the whole therapeutic setting have to meet requirements which have not the same importance in adults.

Up to now, metallic materials like stainless steel, titanium and its alloys are used as wires, screws, plates, intramedullary nails or external fixators as osteosynthesis material in surgical fracture treatment [17]. Correct mechanical fixation of the fracture like compression and stabilisation of the fracture gap supports the healing process. Even micromovements can stimulate the osteoblast activity and therefore the callus formation. But a too rigid fixation (stress shielding) and absent mechanical load during mineralization of the callus or remodelling can lead to a prolonged healing

or even resorption of the bone.

Further mechanical parameters which influence the fracture healing are dimension, geometry and classification of the fracture as well as the mentioned degree and direction of bone fragment movements [2, 15].

From a medical point of view, the first step in fracture treatment is the reduction of the bone to the correct alignment usually under anaesthesia suitable for children. This should happen as soon as possible to minimise the risk of malposition or deformity. Depending on the severity of the injury, closed repositions like a controlled pull along the longitudinal axis or bending and other manipulations of the limb are performed to re-align the bony fragments to their normal anatomical position. In some cases, an open reposition is needed wherein surgically the fracture fragments are exposed by dissecting the tissues. Especially when a fracture has to be surgically stabilised or displacement of the bony fragments cannot be reduced in a closed way. The accuracy of reduction has to be verified by clinical tests like x-ray, especially in case of dislocations close to the growth plate.

Once the fragments are reduced, the reduction is stabilised with an applied casts, traction or fixed by plates, screws, or other external or internal implants [18].

According to Marzi "*The objectives of each fracture treatment are always:*

- o *Minimising the pain,*
- o *Stabilisation of the fracture,*
- o *Small/ short lasting functional limitations,*
- o *Definitive therapy,*
- o *Minimal effort,*

- o *Rapid healing and*
- o *Avoidance of growth disturbances."* [1]

### 1.3.1 Conservative treatment

Per definition, conservative treatment does not include any surgical operation or intervention. Usually, the application of a cast or traction should stabilise, hold and straighten a broken bones or encasing a limb until healing is confirmed.

Indications for conservative fracture treatment are:

- Stable fractures: Greenstick fractures, metaphyseal buckling fractures, slightly dislocated Salter Harris Typ I and II fractures of the distal metaphysis, undislocated joint fractures
- Instable fractures: After reduction and sufficient stability

### 1.3.2 Surgical treatment

Osteosynthesis is defined as reduction and internal fixation of a bone fracture with metallic medical devices [19]. Usually, surgical treatment of bone fractures is carried out if conservative treatment failed or would not stabilise the fracture sufficiently. There are different systems of internal fracture fixation:

- Wire osteosynthesis also known as Kirschner wires (see figure 1.4 a)
- Screw fixation (see figure 1.4 b)
- Tension band wiring (see figure 1.4 c)

## 1 Introduction

---

- Plate osteosynthesis (see figure 1.4 d)
- Intramedullary nails like elastic stable intramedullary nailing - ESIN (see figure 1.4 e)

In children, internal stabilisation of bones and lag screw fixation are the most common methods for osteosynthesis.



Figure 1.4: Examples of a) Wire osteosynthesis, b) Screw fixation, c) Tension band wiring, d) Plate osteosynthesis and e) ESIN fixation [2]

In a growing skeleton, the healing process is faster than in adults, so implants require constant monitoring and sooner explantation. Also the ossification of bones takes

place during childhood and the mechanical properties of the bone depend on the biological age of the child. As long as the closure of the epiphyseal growth plate has not taken place, fractures and other irritations like surgery and improperly used implants may damage the growing bone and can result in growth irregularities [20, 21].

### 1.4 Bioresorbable materials

The development of osteosynthesis materials has been co-continuous with the improvement of the bone fixation knowledge and the complexity of surgical procedures. For load bearing applications currently used implants are made out of stainless steel or titanium requiring implant removal after bone healing [5]. The patient has to undergo an additional operation bearing the risk of possible infections, removal problems of jammed implants, implant migration and last but not least causing extra costs for the health care system.

In recent years, different biodegradable materials were investigated for their use as implants in human medicine. As new approaches in osteosynthesis, they make implant removal unnecessary which would, especially in children, be of crucial benefit for the patient. In children, internal stabilisation of bones and lag screw fixation are the most common methods for osteosynthesis. Up to now, pins and screws made of stainless steel or titanium require a second surgical intervention for implant removal after fracture consolidation. Second to implant removal, these implants lead to a very rigid fixation of fractures preventing micro-movements thus, leading to mild osteoporosis in case of long-time stabilisation [5]. Beside the potential to avoid a second operation, also better biocompatibility and good cell and tissue reactions are known as main properties of biodegradable materials [22]. Therefore, many research groups considered as possible biodegradable implants magnesium and iron

metal and its alloys, calcium phosphate ceramics and polymers [23, 24, 25, 26] like poly(hydroxyl alkanoate), poly (glycolic acid) PGA and poly (lactic acid) PLA and its composites. For several medical applications, these polymers have been FDA approved, but none of them has been successfully processed and modified into strong fixation devices [27]. With some synthetic polymer implants also adverse tissue reactions have been observed [28]. Because of pH changes in the environmental tissue and a degradation rate of about 18 years in the body made another group of polymer interesting: Poly(hydroxyl alkanoate) PHA and especially poly( $\beta$ -hydroxy butyrate) PHB. PHB is gathered renewable from bacteria, but the production and extraction to receive the polymer endotoxin free is complicated. In the last years, the purification process was improved to such a high level that an application as medical device is possible [29]. The interaction of PHB with bone is reported to be promising and it seems to have a huge potential in variation of properties and application [30]. The degradation rate should be faster than that of synthetic polymers [31] and adverse tissue reactions like inflammatory response to the decomposition process can be excluded, because PHB degrades without pH changing. Also the degradation products are getting part of the citric acid cycle and therefore not remaining in the surrounding tissue [32]. On account of this, PHB is chosen for further investigation in different modifications.

### 1.4.1 Requirements bioresorbable materials in children

The beneficial biomechanical properties of novel biodegradable implants were already mentioned in the section above. Due to a too rigid fixation of the fractures, stress shielding [26] and possible mild osteoporosis in case of long-time stabilisation [33] can be avoided.

Beside this mechanical parameters, also biocompatibility and tolerance of degradation

products within the growing body have to be taken into account:

Endotoxin and solvent free production routes are of highest importance to avoid an initial inflammatory response [34, 35]. PLA can be produced from petrochemicals resulting in a racemic mixture. Therefore, many investigations focus on a biological route to produce polymers like PLA [35] or PHAs [34]. Microorganisms process glucose or starch in response to physiological stress like nutrient limited conditions to energy storage polymers. The key steps are the isolation and purification of these bacterial polymers especially in medical application [36].

Resorbable biomaterials are not chemically and biologically inert which leads to regulatory implications [37]: Biocompatibility includes not only the first immune response to the material after implantation, also the degradation behaviour and physiologically acceptable degradation products are of interest [38]. That's why the inflammatory late response, foreign body reaction [39] or oxidative stress in tissue caused by degradation products should be evaluated and predicted to prevent any kinds of adverse effects in children [40, 41].

Beside the already mentioned demanding properties and requirements a bioresorbable material has to meet as an pediatric implant, also the ethical respect of treating vulnerable people has to be considered [42, 43]. Children receive particular attention because by regulatory definition, they have not reached the legal age for consent to treatments involved in research. Developmental limitations, the imbalance within adults and children and the unique terms considering the assent of children and the consent of their parents make the participation of children quite complex. Children need a full disclosure and clear descriptions about treatment and possibilities to receive their understanding and willingness to participate [44, 45]. Clinical trials performed in children are a sensitive topic and although guidelines exist, ethical considerations about risk compared to benefit in accordance with reasonable measures

have to be reviewed [46].

## 1.5 Aims of this thesis

Regarding the challenges of treatment with bioresorbable materials in paediatric trauma care, the three following aims were defined for this thesis:

### 1.5.1 Aim 1) In vivo degradation of novel bioresorbable composites in the femur of rats

Replacing conventional osteosynthesis materials by biodegradable ones is of great benefit and has already gained a rising interest in the recent years [5, 22]. While some interesting implants have only reached experimental status, others, such as polymers like PLA and PGA have already found their way to clinical application. PLA and PGA are FDA approved [27], but their biocompatibility is critical. There are reports about the accumulation of resorption products causing undesirable short and long term soft tissue reactions [47]. Even adverse tissue reactions due pH changes in the environmental tissue and the degradation rate of about 18 years in the body have been observed [28]. Also the complement activation potential of PLA and a high frequency of long-term postoperative inflammatory signs are demonstrated [48]. Overcoming these negative effects, PHB (poly( $\beta$ -hydroxybutyrate)) seems to be a promising candidate for the use as biodegradable material in the human body.

The aim of this study was to investigate the in vivo degradation behaviour of five different PHB composites. The additives were chosen to enhance the degradation time (Herafill<sup>®</sup> and magnesium powder) and the radiological visibility within the micro CT device (Zircondioxide).

### **1.5.2 Aim 2) Biocompatibility and osteoinductive properties of PHB bone implants**

Degradable polymeric materials have to have matching mechanical properties close to the bone to prevent stress shielding [49, 26] and safety of degradation products have to be ensured. The far better biocompatibility of PHB seems to be already ensured [32]: Adverse tissue reactions like inflammatory response to the degradation process are excluded because PHB is reduced in a living organism by hydrolysis [50] and enzymatic degradation [32, 31]. The degradation products of PHB are less acidic compared to PLA and PGA do not remain in the surrounding tissue [32]. In further application, osseointegration and bone-implant interface behaviour are highly influenced by stiffness, strength and damage response of polylactide and hydroxybutyrate implants [4, 51].

The aim of this study was to investigate the bone tissue reaction and the mechanical behaviour of five different PHB composites. The additives were chosen to enhance the degradation time (Herafill<sup>®</sup> and magnesium powder) and the radiological visibility within the micro CT device (Zircon dioxide).

### **1.5.3 Aim 3) Immunological response to bone injuries and implantation of a biodegradable polymer**

In former studies implanted subcutaneously, PHB showed good tissue tolerance, no acute inflammation or tissue necrosis or other adverse reactions in the surrounding tissue. But also like PLA, some mild inflammatory reactions and fibrous encapsulation occurred during the first few weeks of implantation which were referred to impurities of the material [24]. PLA in close contact to blood, plasma or intestinal

fluid, showed that this inflammatory effect can be much higher [48]. Because of these reports, there is much research on the investigation of new production and processing routes, to enhance the purification of PHB and the cleaning steps for further endotoxin removal [52, 34, 29]. These impurities and endotoxins in the material are often the reasons for adverse tissue reactions, fibrous encapsulations or acute and long-term response of the immune system. In this cases, the early steps of defence are the non-specific or innate immune system. It reacts against any kind of microbial and infectious „non-self“ and initiates the process leading to an eventual development of an adaptive immune response and establishment of an immunological memory. As an essential component of the innate immune system, the phagocyte system (like macrophages, monocytes and neutrophils) performs various defence functions that rely on the phagocytic uptake and digestion of pathogens. Adequate numbers of monocytes and neutrophils need to be present in the peripheral blood to ensure an efficient function. But also responding to signals from the site of inflammation, migration and ingestion of the invaded microorganisms are required.

Because of the novel production possibilities, higher purity of PHB and a lack of detailed information about the immunological response to implanted PHB, the aim of this study was to investigate the impact of PHB to the innate immune system in a living rat model with the specific focus on the phagocytic activity of these cells.

## 2 Materials and Methods

### 2.1 Implants

In this thesis, cylindrical pins made of *Poly(3-hydroxybutyrate)* (PHB) which belongs to the group of bio-polymers gathered from the cytoplasm of the bacteria *Escherichia coli* [53] with different additives were analysed: pure PHB, PHB with 3w% Zircondioxid, PHB with 3w% Zircondioxid and 30w% Herafill<sup>®</sup>, an alternative bone material, PHB only with 30w% Herafill<sup>®</sup> and PHB with 40w% Magnesium powder (44  $\mu\text{m}$  particle size). The used implant materials and their compounds are listed in table 2.1.

Composite	PHB	Herafill <sup>®</sup>	ZrO <sub>2</sub>	Mg powder
	weight %	weight %	weight %	weight %
P	100	0	0	0
P3Z	97	0	3	0
P30H	70	30	0	0
P3Z30H	67	30	3	0
P40Mg	60	0	0	40

Table 2.1: PHB composite materials used in this study.

The composites containing 3w% ZrO<sub>2</sub>, which is known to absorb X-rays, are designed to increase the radiological contrast values [54], is chemically inert and did not show any significant toxicity to bone cells [55]. 30w% Herafill<sup>®</sup> (Heraeus, Wehrheim, Germany) were added to increase the degradation rates compared to native PHB. As a composite of calcium sulphate (CaSO<sub>4</sub>), calcium carbonate (CaCO<sub>3</sub>) and glycerol tripalmitate, Herafill<sup>®</sup> is used as an alternative bone substitute material because of its good osteoconductivity properties [56]. Particles with a grain size of several µm were used within the PHB composites, but biocompatibility was not tested at this stage. The biomechanical parameters of PHB composites were evaluated at the Vienna University of Technology in former studies [4] (see table 2.2).

Composite	Young's Modulus	Elongation at Fracture	Tensile Strength
	GPa	%	MPa
P	3.0	3-4	37.6
P3Z	2.3	3	25
P3Z30H	2.8	2-3	25.3
P30H	-	-	-
P40Mg	3.7	1	30
PGA	7	15-20	340-920
PLLA	2.7	5-10	80-500
PLGA	2.0	3-10	40-55

Table 2.2: Biomechanical properties of PHB composites [4] compared to biomechanical properties of PGA, PLLA and PLGA screws [5]

All implants were 1.6 mm in diameter and 8 mm in length see figure 2.1. The polymer was produced and purified by the Technical University of Graz, Dr.rer.nat. Koller. The implants were injection-molded using a Haake MiniLab Micro Compounder and extruded into a mold in the DSM Research 3.5 mL Injection Molding Machine at

the Technical University of Graz, Dr.rer.nat. Clemens Ebner. The Zircondioxide, Herafill<sup>®</sup> or Magnesium powder was added to the PHB homopolymer during the processing step. The processing and injection molding parameters were adjusted to the specifications of the material used in order to yield perfectly shaped molds without defects or gas inclusions. All produced pins were implanted in the femur of growing Sprague Dawley<sup>®</sup> rats to investigate and relate the biodegradable properties of these different materials in an *in vivo* rat model.

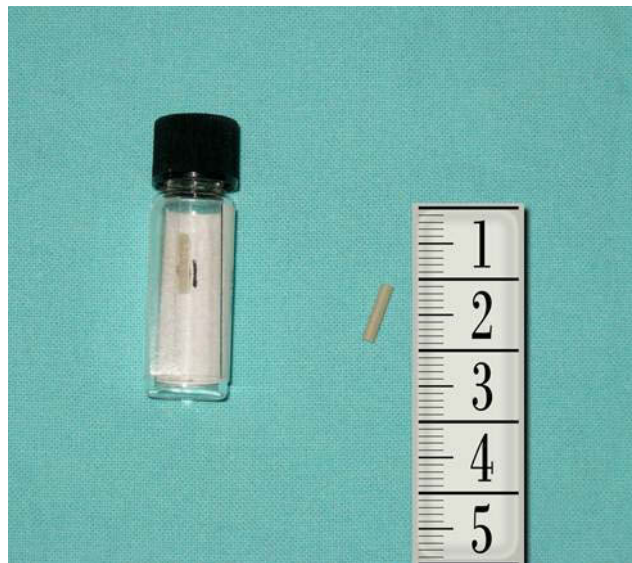


Figure 2.1: native PHB Implant

## 2.2 Experimental design

Male Sprague Dawley<sup>®</sup> rats with a body weight of 120 – 160 g and 5 weeks of age were used and divided in two different studies depending on the carried out examinations:

### The continuous- micro CT study

In this study, 108 rats were divided in five different groups and got two identical pins of native PHB and PHB with or without Zircondioxid, with Herafill<sup>®</sup> or with Mg powder (6 rats per material composite group and time point, see table 2.3) implanted into its femoral bones (see figure 2.2). The continuous- microCT group underwent micro CT evaluation at the seventh day after operation followed by further micro CT examinations after 1, 3, 6 and 9 months. Except for the PHB and the PHB with Herafill<sup>®</sup> groups, they have been terminated after 6 months because the contrast between implant and environmental tissue was too low to evaluate the degradation behaviour of the material. At the end of the study, the animals were euthanized, the bones explanted and also implants removed for further high resolution microCT scans.

	Group	P	P3Z	P3Z30H	P30H	P40M
	Time	PHB	PHBZrO <sub>2</sub>	PHBZrO <sub>2</sub> Herafill <sup>®</sup>	PHBHerafill <sup>®</sup>	PHBMg
<b>n</b>	1 M	6	6	6	6	6
<b>n</b>	3 M	6	6	6	6	6
<b>n</b>	6 M	6	6	6	6	6
<b>n</b>	9 M	-	6	6	6	-

Table 2.3: Experimental procedure divided in five groups: P = native PHB, P3Z = PHB with 3w% Zircondioxid, P3Z30H = PHB with 3w% Zircondioxid and 30w% Herafill<sup>®</sup>, P30H = PHB with 30w% Herafill<sup>®</sup> and P40M = PHB with 40w% Magnesium powder

At each time point after 1, 3 and 6 months, 6 animals were euthanized and the bones explanted to embed them and perform histological slices.

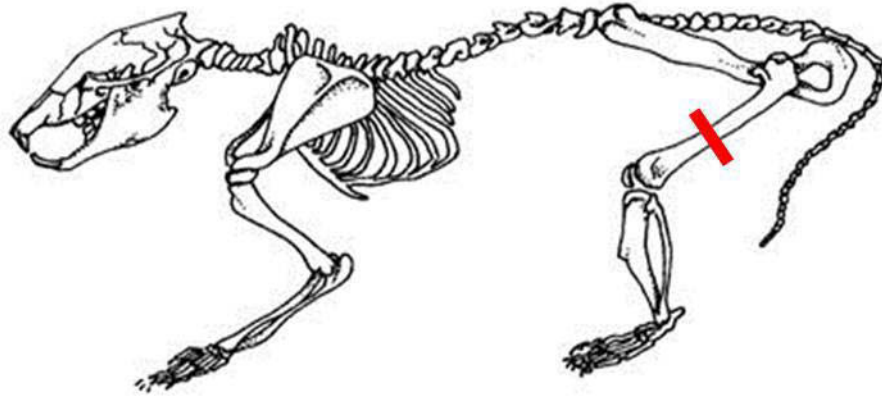


Figure 2.2: Bilateral transcortical implantation of pins of different PHB composites

### **The immunological study**

In this study, 18 rats were divided in three groups: The experimental group (B) received a transcortical drill-hole through the femoral shaft and the bioresorbable implant of *Poly(3-hydroxybutyrate)* PHB. Each rat got two identical pins of PHB implanted into its femoral bones. The Sham group (S) was limited to the drill-hole 1.5 mm in diameter and the control group (C) did not undergo any surgical procedure. Detailed information is presented in table 2.4. Blood samples were collected before operation, weekly in the first four postoperative weeks and after 8 weeks. All groups underwent microCT evaluation at the seventh day after operation followed by further microCT examinations after 4 and 8 weeks.

Group	B	S	C
Implant	PHB with 3w% ZrO <sub>2</sub>	no	no
Surgery	drill hole	drill hole	untreated
n	6	6	6

Table 2.4: Experimental procedure in groups: B = Experimental group with PHB, S = Sham group, C = Control group

## 2.3 Ethical approval

All animal experiments were conducted under animal ethical respect and were authorised by the Austrian Ministry of Science and Research (accreditation number BMWF-66.010/0070-II/3b/2011). Rats were housed in groups of four in clear plastic cages on standard bedding. Water and a standard pellet diet were given ad libidum. The animals were under daily observation of certified animal care taker and veterinarian. The ethical approval is attached to the "*Appendices*" section.

## 2.4 Surgical procedure

Volatile isoflurane (Forane<sup>®</sup>, Abbot AG, Baar, Switzerland) was administered for general anaesthesia preceded by a subcutaneous combined sedation, administering a mixture of Fentanyl (20 µg/kg Fentanyl<sup>®</sup>, Janssen-Cilag GmbH, Neuss, Germany), Midazolam (400 µg/kg Midazolam Delta<sup>®</sup>, DeltaSelect GmbH, Dreieich, Germany) and Medetomidine (200 µg/kg Domitor<sup>®</sup>, Pfizer Corporation Austria GmbH, Vienna, Austria). The mid-diaphyseal region of the femur was exposed through a lateral approach. A drill (1.5 mm) with ascending diameter (Synthes<sup>®</sup>, Paoli, PA,

USA) was used to prepare the transcortical implantation bed with the longitudinal axis of the drill hole perpendicular to the longitudinal axis of the femoral diaphysis. After transcortical placement was ensured, the operating field was irrigated thoroughly with physiological saline solution and the wound was closed [57] (whole procedure see figure 2.3).

The general anaesthesia was antagonised by an intraperitoneal injection of a mixture of Naloxone (120 µg/kg; Narcanti<sup>®</sup>, Torrex Chiesi Pharma GmbH, Vienna, Austria), Flumazenil (50 µg/kg; Anexate<sup>®</sup>, Roche Austria GmbH, Vienna, Austria) and Atipamezole (250 µg/kg; Antisedan<sup>®</sup>, Pfizer Corporation, Vienna, Austria). Postoperatively, all animals received 200 mg/kg Caprofen (Rimadyl<sup>®</sup>, Pfizer Corporation, Vienna, Austria) which was injected subcutaneously on the operation day to ensure analgesia. During the first postoperative week, analgesia was maintained by administration of 60 mg Piritramid (Dipidolor<sup>®</sup>; Janssen-Cilag GmbH, Neuss, Germany) in 25 ml 5% glucose added to 500 ml drinking water. The rats were allowed to move freely in their cages without external support and unrestricted weight bearing. Daily clinical observation was performed throughout the study period [57].

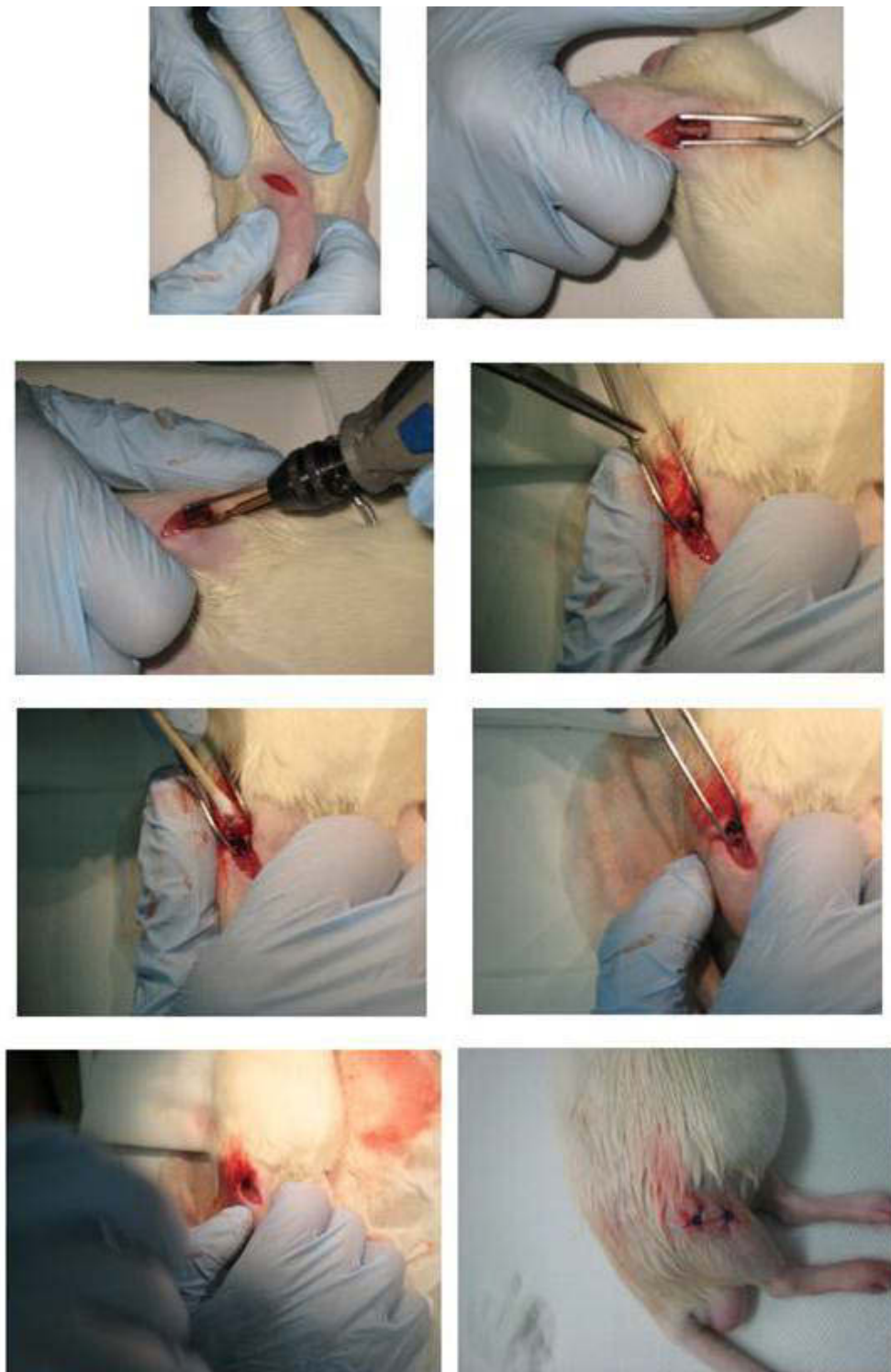


Figure 2.3: Surgical procedure of transcortical implantation in the femur of rats (friendly courtesy of Dr.med.univ. K. Angerpointner) [3]

## 2.5 Blood sampling

Rats of the immunological study underwent a volatile isoflurane (Forane<sup>®</sup>, Abbot AG, Baar, Switzerland) anaesthesia. One of the two tongue veins (*Vena lingualis*) was punctured using a 20-gauge needle (Sterican<sup>®</sup>) as seen in figure 2.4. 1 ml of blood was drawn into lithium-heparin coated tubes. In order to avoid blood coagulation, 250 I.E. Heparin (Heparin Immuno<sup>®</sup>, Ebewe Pharma, Sandoz, Austria) was added to each sample. Contaminations of saliva are possible with this blood sampling method. The samples were collected before operation, weekly in the first four postoperative weeks and after 8 weeks. Some of the blood examinations were performed by Dr.med.univ. Katharina Angerpointner within her diploma thesis [3].

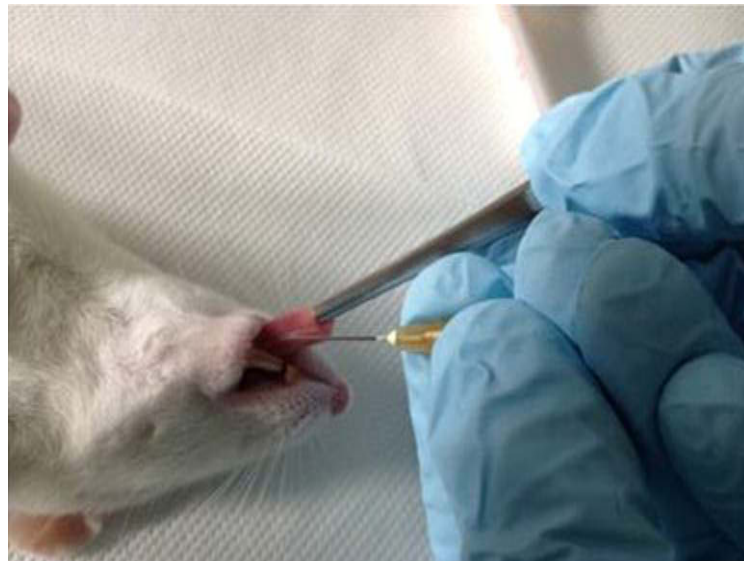


Figure 2.4: Blood sampling through tongue veins

## 2.6 Phagocytic assay

After blood sampling, the phagocytic activity of neutrophils was determined in the lab of Prof. Dr. Brezinsek (Division of Rheumatology and Immunology, Medical University of Graz) using the Phagotest kit (Opregen Pharma, Heidelberg, Germany). In this test, phagocytes in heparinized whole blood (100  $\mu$ l) were incubated with FITC-labelled E. Coli ( $2 \times 10^7$  per 20  $\mu$ l at 37°C for 10 min) for ingestion. The phagocytosis was stopped by setting the samples on ice and quenching solution (100  $\mu$ l) was added to eliminate the fluorescence of non-phagocytosed bacteria. After two washing steps (3 ml washing solution, 5 min, 250 x g, 4°C) the cells were re-suspended and incubated (2 ml lysis solution, 20 min) to lyse erythrocytes and fix the leukocytes. After the final washing step (3 ml washing solution, 5 min 250 x g, 4°C) the cells were re-suspended in DNA staining solution (200  $\mu$ l) to exclude aggregation artefacts of bacteria or cells. The phagocytes are able to digest the bacteria, the green fluorescence signal of FITC (Fluorescein isothiocyanate) can be quantified by flow cytometry [58]. In parallel a negative control was kept on ice. The test was performed according to the manufacturer's instructions.

## 2.7 Flow cytometric analysis

The phagocytic ability was evaluated in neutrophil granulocytes. The analysis was performed using a FACSCanto II<sup>®</sup> flow cytometer (BD Biosciences, Heidelberg, Germany) and the data were processed with the FACSDiva 6.1.3<sup>®</sup> software (BD Bioscience). A gate was set in the red fluorescence histogram on those events which had the same DNA content as a rat diploid cell to exclude extracellular bacteria. In the FCS vs SSC scatter diagram, dead cells were excluded. Live populations were gated by the software program in the scatter diagram (FCS vs SSC) and their

green fluorescence histogram was analysed. The phagocytic ability was expressed as percentage of fluorescent cells in the total population studied and calculated by subtracting the percentage of the negative control sample (<1%) from the positive control sample [20].

### 2.8 Euthanasia

For euthanasia volatile isoflurane (Forane<sup>®</sup>, Abbot AG, Baar, Switzerland) was used for general anaesthesia. Subsequently, 25 mg sodium thiopental (Thiopental<sup>®</sup> Sandoz, Sandoz GmbH, Kundl, Austria) was injected into the cardiac ventricle, leading to immediate cardiac arrest. Immediately after harvesting the femur, all soft tissues were carefully removed and freeze-dried at -80°C [57].

### 2.9 Microfocus computed tomography *in vivo*

Microfocus computed tomography ( $\mu$ CT) is an emerging technology that combines both noninvasive tissue-preserving imaging and quantitative morphometry of bone structure in three dimensions [59, 60]. During the  $\mu$ CT examinations the animals were generally anaesthetised by volatile isoflurane (Forane<sup>®</sup>, Abbot AG, Baar, Switzerland). The rats were scanned using the software Siemens Inveon Acquisition Workplace 1.2.2.2. Scans were made at 70 kV voltage, 500  $\mu$ A current, and 1000 ms exposure time. Rotation of 210° by 180 rotation steps led to a resolution of the whole femoral bone with an effective pixel size of 35.55  $\mu$ m. For reconstruction a down-sample factor of 1 was used. The system allowed the 3D reconstruction of a specimen from a set of 2D projections using the back projection of a filtered projection algorithm. The scanned datasets were converted into DICOM format

and as such imported into the medical image processing software Mimics<sup>®</sup> (Version 14.0, Materialise NV, Leuven, Belgium), constructing a 3D model of the pin through image processing and 3D reconstruction technologies. 3D pin-bone surface models were also extracted from the  $\mu$ CT images, using the optimal parameter settings. The volume of interest was defined for each part using region-growing of determined Hounsfield units (HU) and manual drawing of bone-implant contours at the cortical sites [57]. Pin volume and pin surface were calculated and the quantification of bone tissue formation was measured within an area of 250  $\mu$ m around the implant. With the Mimics<sup>®</sup> program, a circle with repeatable distance from the implant surface can be drawn and the bone volume within this circle quantified (see figure 2.5). Bone to tissue volume was calculated with the following equation:

$$\frac{BV}{TV} = \frac{measuredBV}{(r^2_{TCROI} \times \pi \times h_{roi}) - (r^2_{TCImplant} \times \pi \times h_{ROI})} \quad (2.1)$$

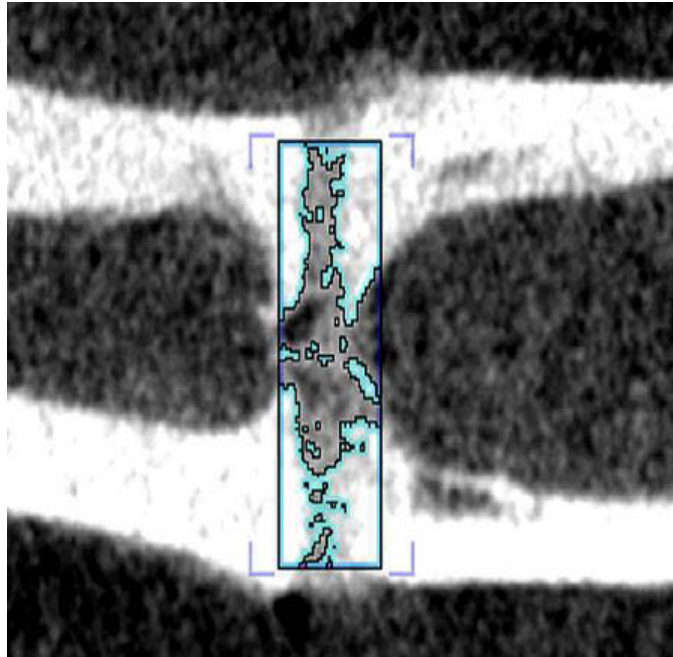


Figure 2.5: After 6 months of implantation, PHB with 30w% Herafill<sup>®</sup> calculation of BV/TV with MIMICS<sup>®</sup>

Dr.med.univ. Jan Weigel calculated and analysed the bone and tissue volume of the different PHB composites within his diploma thesis [61].

## 2.10 Microfocus computed tomography *ex vivo* high resolution

The deep frozen bones were scanned with  $\mu$ CT using a polychromatic source at 80 kV voltage, 500  $\mu$ A current with an exposure time of 2000 ms and an effective pixel size of 19.17  $\mu$ m. Scanning was performed with no storage trays on de-wrapped samples. Images were reconstructed using the Siemens Inveon<sup>™</sup> Workplace 3.0 software and a filtered back projection with a bilinear interpolation and a Shepp–Logan filter

were applied. Pins were reconstructed as three-dimensional (3D) models, and upper and lower thresholds for the pins were set at 3256 and 8064 Hounsfield units (HU). Dr.med.univ. Gustav Schmöller performed *ex vivo* high resolution scans within his diploma thesis [62].

### 2.11 Push out tests

The push out experiments were performed at the Vienna University of Technology from Dr. Anna Celarek. The harvested bones were kept frozen (-20°C) and thawed at least one hour before testing. Prior to mechanical testing, all samples were photographed with an optical microscope for visual assessment of the implant and bone (see figure 2.6a). The pin was displaced by pressing a cylindrical steel rod with 1 mm in diameter with constant velocity of 1 mm/min vertically against the pin. A detailed description of the method is published in Celarek et al. [4] (see figure 2.6b,c). The force is plotted versus the pin displacement to determine shear strength, fracture energy and stiffness are determined as followed:

The shear strength is calculated by dividing the force maximum (point of failure) by the area of the implant bone interface. The integral of the force of the displacement from 0 to 0.5 mm defines the fracture energy and the slope the interface stiffness. The pin is classified as loosened, if it could be pushed out gently by hand, or if the shear strength is below  $0.1 \text{ N/mm}^2$  and, in addition, the fracture energy below 0.5 mJ [4].

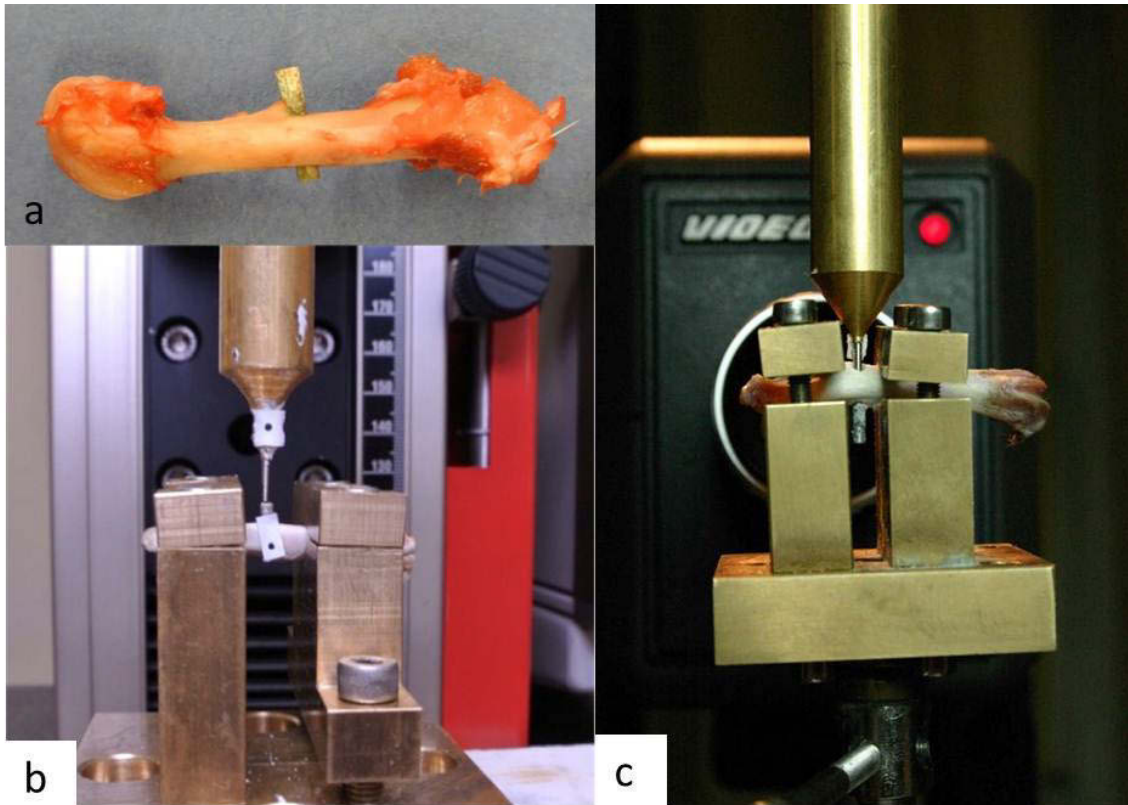


Figure 2.6: Push out tests: a) Optical assessment of the implant b,c) Experimental setup for mechanical pin displacement

## 2.12 Histological sample processing

The explanted bones were dissected from soft tissues and fixed in neutral buffered 4% formalin solution. The region of interest was excised using a high-precision saw (Exakt Apparatebau, Norderstedt, Germany). The samples were dehydrated in ascending grades of alcohol and embedded in light-curing resin (Technovit 7200 VLC, Kulzer & Co., Hanau, Germany). The blocks were processed with the Exakt Cutting and Grinding Equipment (Exakt Apparatebau, Norderstaedt, Germany)

according to Donath [63]. Thin ground sections were prepared through the central axis of the implant and parallel to the longitudinal axis of the femur shaft. Slices were reduced to a thickness of 30  $\mu\text{m}$  and stained with Levai–Laczko dye [57]. Digital virtual microscopic overview images at a 200x magnification were produced with an Olympus dotSlide Microscopic system (dotSlide – Virtual Slide System, Olympus, Japan). On these histological slices, the whole length of implant in the bone and the lengths of bone cells (brown/grey cells in the figures 2.7 marked with red arrows) in contact to the implant were measured. So the percentage of bone adherence on the implant length can be calculated. The quantification of bone adherence was measured by ImageJ<sup>®</sup> (open source, Wayne Rasband, Maryland, USA).

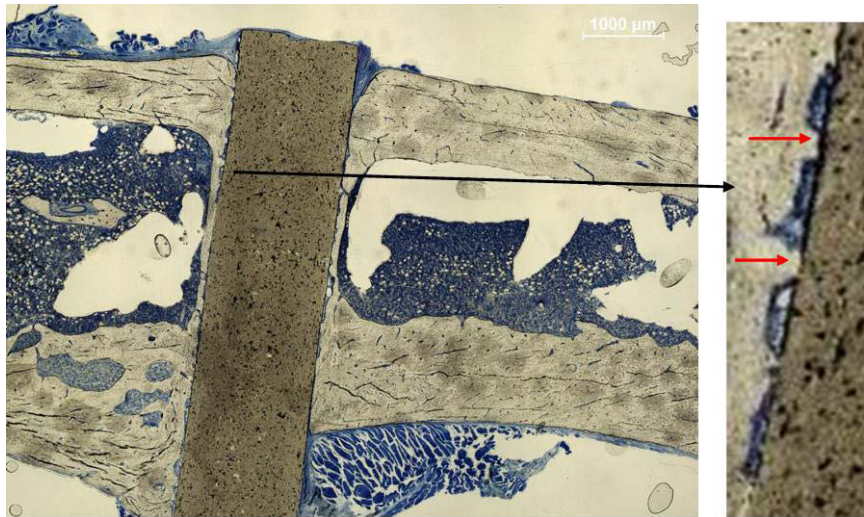


Figure 2.7: Histological slice of PHB with Zirconium dioxide and Herafill<sup>®</sup> after 6 months. The red arrows indicate bone adherence.

## 2.13 Statistics

For statistical analysis, SPSS 21 (SPSS Inc., Chicago, IL, USA) was used. For comparison of the different time points within a group the Kruskal-Wallis test was applied, as data was limited to six samples each time point. The non-parametric Wilcoxon Test was used to compare differences between two groups. Values were expressed as means with standard deviations (SD) and ranges. A p-value  $<0.05$  was considered to be statistically significant.

### 3 Results

The animals tolerated full weight bearing post operationem. Clinically, all animals showed slight reddening of the wound, as well as mild wound swelling resulting from surgery. However, no wound infections can be observed.



Figure 3.1: 3D reconstruction of bone with native PHB implant, unseen because of similar density like environmental tissue

Because of similar density of PHB and the environmental tissue, the  $\mu$ CT analysis was inconclusive in calculating the degradation of implanted native PHB pins (see figure 3.1 and 3.2).

The  $\mu$ CT scans were stopped after 6 months because in case of PHB the degradation

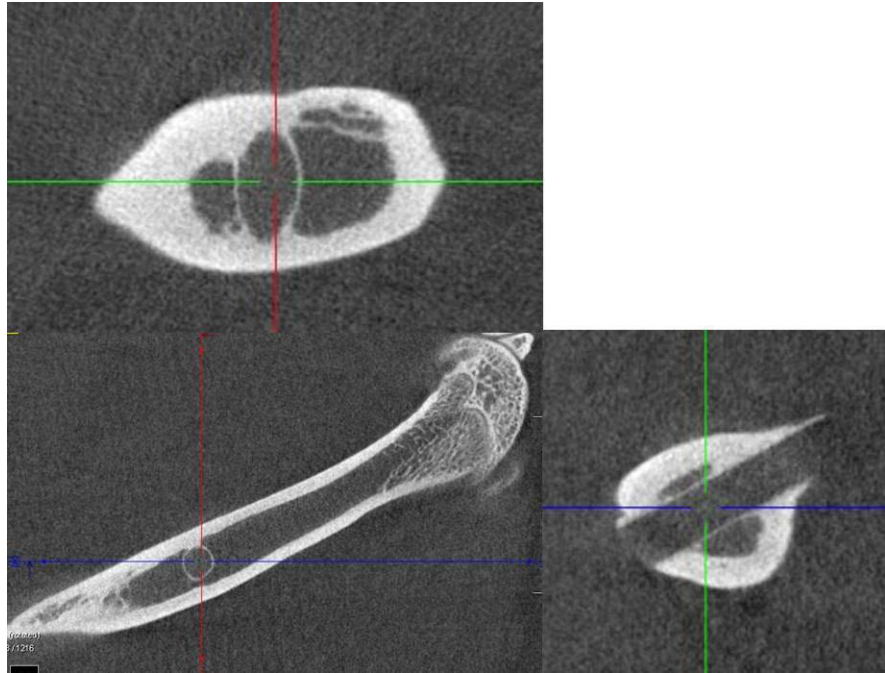


Figure 3.2: native PHB implanted into the femur of rats, only new formed bone around the implant is visible in 2D reconstruction

process could not be visualised. Therefore, to get a better contrast between tissue and implant, 3w% Zircondioxid was added to PHB. Also degradation process and strength of PHB were too low. So, to improve these properties, 40w% Magnesium powder and 30w% Herafill<sup>®</sup> were added too. Herafill<sup>®</sup> is an alternative bone material from Heraeus Medical Group (Wehrheim, Germany) and should enhance the degradation process of PHB and the bone adhesion on the surface of the implants.

Magnesium is known to be osteoinductive and because of its faster degradation performance as  $\text{Mg} + \text{H}_2\text{O} \rightarrow \text{Mg}(\text{OH})_2 + \text{H}_2\uparrow$  it was mixed with PHB to accelerate the degradation rate.

Initially, tensile tests were performed to quantify the influence of Mg powder on the mechanical properties. Results showed an increase in the Young's modulus with increasing amount of Mg powder, whereas the influence on the tensile strength was

found to be rather low. The addition of 40w% Mg powder caused an increase in the Young's modulus of 20%. The Mg powder did not affect the mechanical strength of the material but the test specimens showed increased brittleness indicated by shorter elongation at break and stress-strain curves. Therefore, some implants were broken during the implantation procedure because of this appeared implants' brittleness.

## 3.1 Aim 1) *In vivo* degradation of novel bioresorbable composites in the femur of rats

PHB with or without Zircondioxid, with Herafill<sup>®</sup> or with Mg powder as pins were successfully implanted in 12 femoral bones in 6 rats each. No rat was lost during the study period and no bone got fractured.

### 3.1.1 Microfocus computed tomography *in vivo*

After implantation, the rats were scanned after 1, 3, 6 and 9 months. The datasets were reconstructed into a filtered projection algorithm and screenshots from 3D and 2D reconstruction from sagittal side were performed to every time point. Figure 3.3 show PHB with 3w% Zircondioxid from month 1, 3, 6 and 9, figure 3.4 with 3w% Zircondioxid and 30w% Herafill<sup>®</sup>, figure 3.5 PHB with 30w% Herafill<sup>®</sup> and figure 3.6 PHB with 40w% Magnesium powder.



Figure 3.3: PHB with 3w% Zircondioxid at different time points of implantation: month 1 (a) sagittal 2D, (e) and 3D reconstruction; month 3 (b) sagittal 2D, (f) and 3D reconstruction; month 6 (c) sagittal 2D, (g) and 3D reconstruction; and month 9 (d) sagittal 2D, (h) and 3D reconstruction



Figure 3.4: PHB with 3w% Zircondioxid and 30w% Herafill<sup>®</sup> at different time points of implantation: month 1 (a) sagittal 2D, (e) and 3D reconstruction; month 3 (b) sagittal 2D, (f) and 3D reconstruction; month 6 (c) sagittal 2D, (g) and 3D reconstruction; and month 9 (d) sagittal 2D, (h) and 3D reconstruction

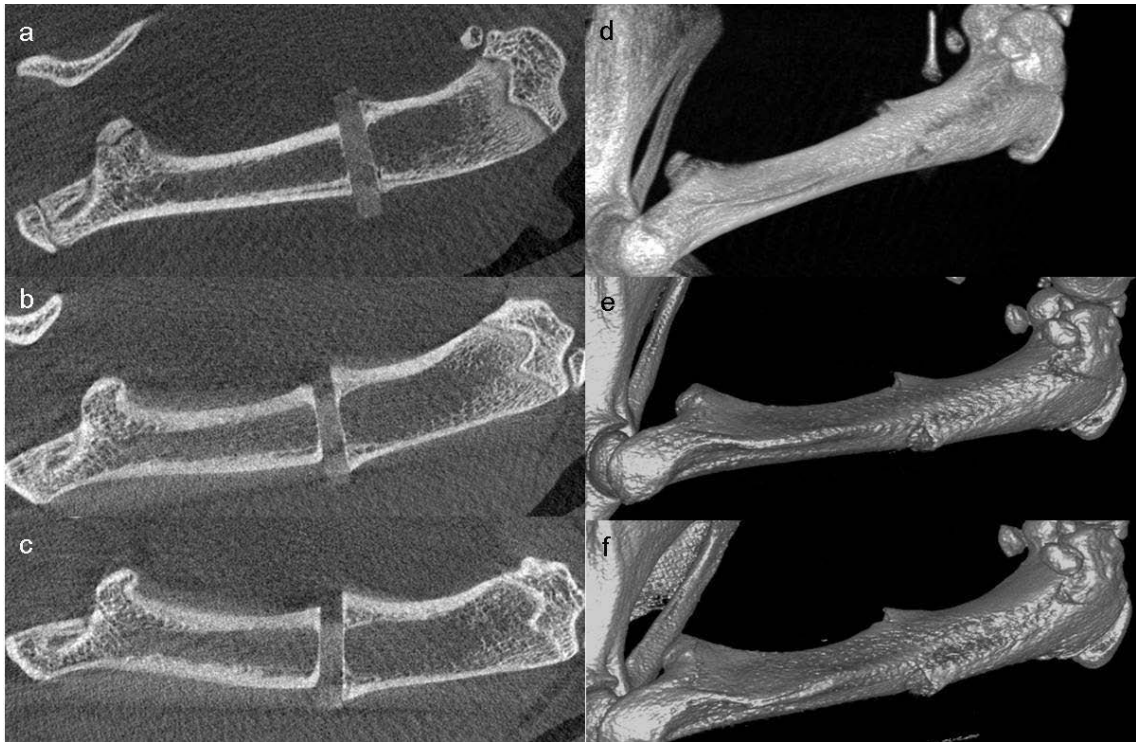


Figure 3.5: PHB with 30w% Herafill® at different time points of implantation: month 1 (a) sagittal 2D, (d) and 3D reconstruction; month 3 (b) sagittal 2D, (e) and 3D reconstruction; and month 6 (c) sagittal 2D, (f) and 3D reconstruction

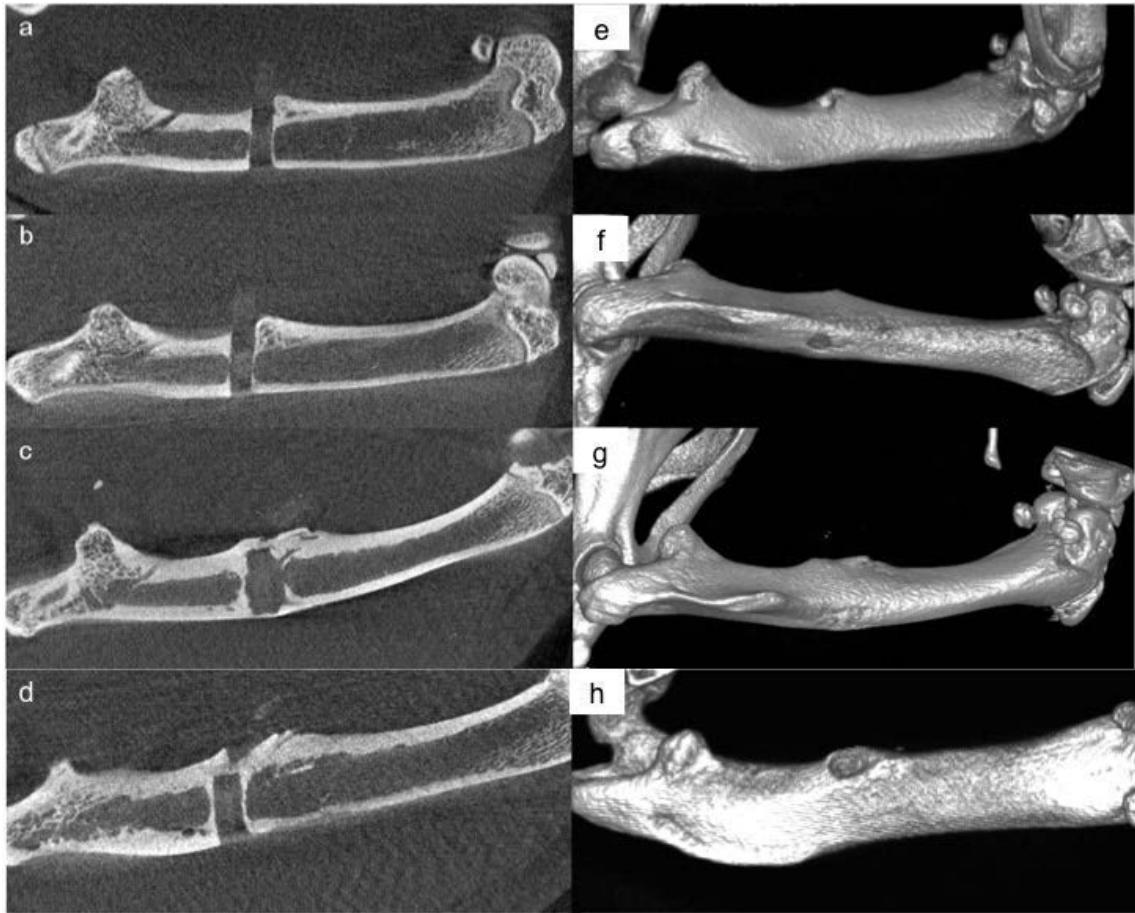


Figure 3.6: PHB with 40w% Magnesium powder at different time points of implantation: month 1 (a) sagittal 2D, (e) and 3D reconstruction; month 3 (b) sagittal 2D, (f) and 3D reconstruction; month 6 (c) sagittal 2D, (g) and 3D reconstruction; and month 9 (d) sagittal 2D, (h) and 3D reconstruction

The reconstructed datasets were converted into DICOM format to import them into a medical image processing software Mimics<sup>®</sup> for volume and surface calculations. The threshold was set for PHB with Zircondioxid between -250 and 400 HU and for PHB with Zircondioxid and Herafill<sup>®</sup> between -160 and 530 HU. With edit mask,

the limits between implant and surface were erased and with region growing, the remaining implant was segmented. Then a 3D implant picture could be drawn and the volume and surface calculated (see figure 3.7). Again, the resolution between implant and surface was not high enough to get valid volume and surface values. In the  $\mu$ CT scans of the first 6 months, it seems that the implant volume was only slightly reduced and the surface increased. But for valid data, the new bone formation on the implant surface (see figure 3.7 the red arrows) disturbed the volume and surface calculation because the limits and edges could not be set repeatable.

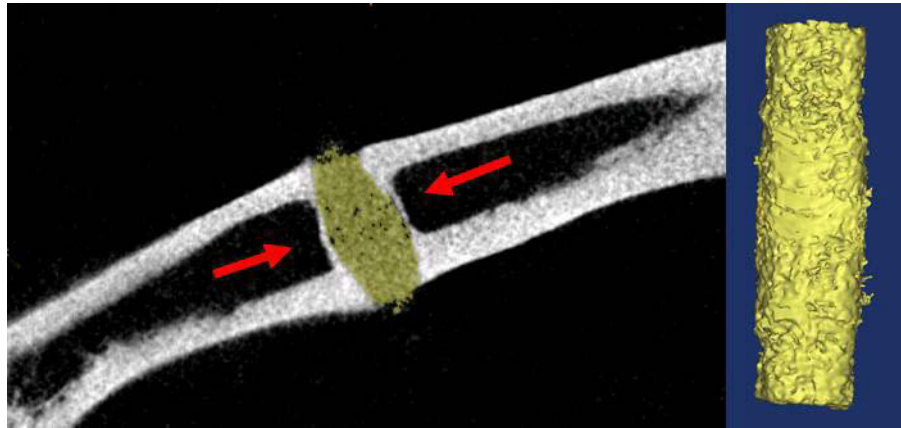


Figure 3.7: In Mimics<sup>®</sup> segmented and calculated volume and surface of P3Z30H implant after 6 months

#### 3.1.2 Microfocus computed tomography high resolution *ex vivo*

9 months after implantation, the animals were euthanized, the bones explanted and deep frozen. Except for the PHB and the PHB with Herafill<sup>®</sup> groups, they have been terminated after 6 months because the contrast between implant and environmental tissue was too low to evaluate the degradation behaviour of the material. During micro CT evaluations, the bones were kept on dry ice to prevent any thawing. Again,

### 3 Results

---

screenshots 2D reconstruction from sagittal side were performed as shown in figure 3.8 PHB with 30w% Herafill<sup>®</sup> and in these high resolution scans, it is clearly visible that there is no remarkable degradation of the implant.

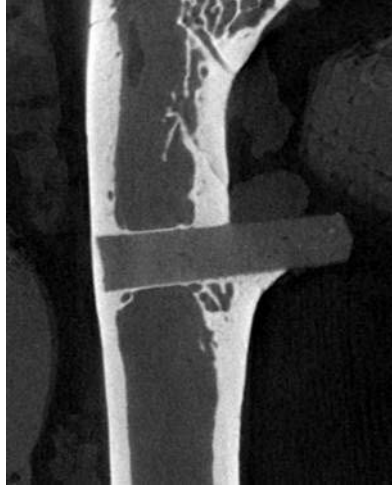


Figure 3.8: High resolution scan of explanted P3Z30H implant after 9 months.

Figure 3.9 is also a high resolution scan of PHB with 40w% Magnesium powder. Here, the added Magnesium powder was degrading faster than the PHB polymer matrix and dissolved partially out of the PHB network. Only in the middle of the implant is a part with higher density where the Magnesium powder still remains (red circle). The implant was too brittle, that's why it broke during the healing process with overgrowing bone reaction. The diameter of the remaining implant was measured to see if the faster degradation of the Magnesium powder also resulted in a faster degradation of the PHB matrix. But the values are between 1.56 and 1.59 mm and the original implant had 1.6 mm in diameter. So again, almost no degradation of the PHB implant can be observed during 9 months of implantation.



Figure 3.9: High resolution scan of explanted P40Mg implant after 9 months with measured diameter and length of implant

Only the 2 composites P3Z and P3Z30H with added zirconium dioxide had good enough contrast in the micro CT scans to evaluate the implant and calculate the implant surface and volume. *Ex vivo* micro CT data after 3, 6 and 9 months of implantation was used and as starting point, the initial pin volume ( $16.09 \text{ mm}^3$ ) and surface ( $44.23 \text{ mm}^2$ ) were calculated. The calculated values are shown in table 3.1 and the longitudinal monitoring demonstrates only minor changes between month 3 and 9. No relevant differences in degradation behaviour can be shown between P3Z and P3Z30H. This is also obvious over the whole study period within all microCT scans, which show an increasing callus formation and bone accumulation around the implant. But an increase of implant volume and surface can be investigated at this two composites (see table 3.1) compared to the calculated basic values. This dwelling

### 3 Results

of the implant was noticeable in both PHB composites (see table 3.2) starting at the first *ex vivo* results in the third month.

Time Months	Composite	Volume $mm^3$			Surface $mm^2$		
		M	R	SD	M	R	SD
	Calculated	16.09	-	-	44.23	-	-
3	P3Z	16.89	15.69 - 17.79	0.877	59.91	53.04 - 81.51	8.866
	P3Z30H	18.16	17.39 - 18.83	0.524	57.89	54.67 - 65.83	4.586
6	P3Z	16.26	14.72 - 17.20	0.914	60.76	55.83 - 63.46	4.689
	P3Z30H	17.98	17.13 - 18.59	0.490	56.62	54.26 - 60.84	2.134
9	P3Z	16.26	14.72 - 17.20	0.914	60.76	55.83 - 63.46	4.689
	P3Z30H	17.98	17.13 - 18.59	0.490	56.62	54.26 - 60.84	2.134

Table 3.1: Measured implant volume and surface with mean values (M), measurement range (R) and standard deviation (SD) after 3, 6 and 9 months *in vivo*. Original implant volume and surface were calculated from a cylindrical shape of 1.6 mm in diameter and a height of 8 mm [6].

Composite	VG 3 M	SG 3 M	VG 6 M	SG 6 M	VG 9 M	SG 9 M
	%	%	%	%	%	%
P3Z	4.9	35.5	1.0	37.4	8.5	35.72
P3Z30H	12.9	30.9	13.6	28.0	13.6	29.9

Table 3.2: Measured percentage of volume gain (VG) and surface gain (SG) after 3, 6 and 9 months [6].

## 3.2 Aim 2) Biocompatibility and osteoinductive properties of PHB bone implants

### 3.2.1 Microfocus computed tomography *in vivo*

The quantification of bone volume formation was measured after 1, 3 and 6 months using the Mimics<sup>®</sup> program. For the different PHB groups, the  $\mu$ CT 3D bone formations are visible in the figures 3.10 to 3.12.

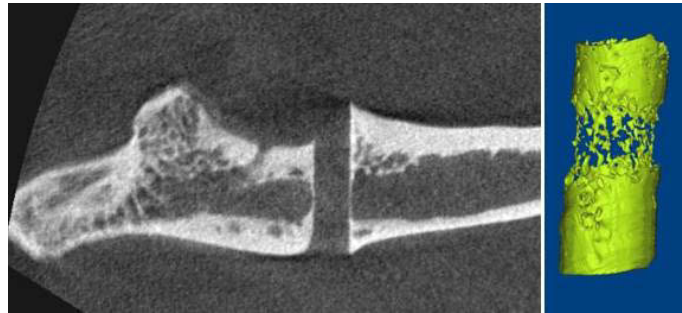


Figure 3.10: 3D bone formation calculated and segmented in Mimics<sup>®</sup> of native PHB after 6 months

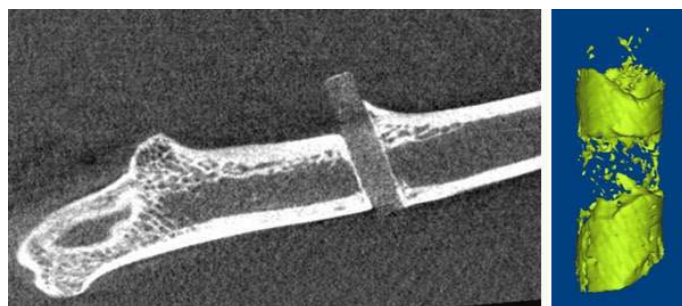


Figure 3.11: 3D bone formation calculated and segmented in Mimics<sup>®</sup> of PHB with Zirconium dioxide after 6 months

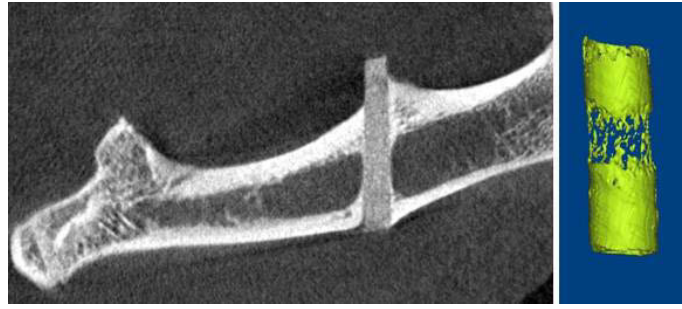


Figure 3.12: 3D bone formation calculated and segmented in Mimics<sup>®</sup> of PHB with Zirconium dioxide and Herafill<sup>®</sup> after 6 months

There are no significant differences between the three composites in the bone volume and native PHB, but PHB with 3w% Zircon and 30w% Herafill<sup>®</sup> shows the highest bone volume values (see table 3.3). During longer implantation time, in all study groups a tendency of decreasing bone volume is visible. Again, no significant differences are within the three composite groups in the calculated bone to tissue volume. But also here, PHB with 3w% Zircon and 30w% Herafill<sup>®</sup> shows the highest bone to tissue volume values (see table 3.3) and the values are decreasing during 9 months of implantation.

Composite	Timepoint	M	SD
months			
P	6	0.42	0.10
P3Z	3	0.32	0.12
	6	0.26	0.14
	9	0.14	0.01
P3Z30H	3	0.51	0.06
	6	0.38	0.09
	9	0.31	0.06
P30H	3	0.39	0.09
	6	0.21	0.08

Table 3.3: Calculated bone volume (BV) to total volume (TV) fraction around the implant.  $N \geq 6$  samples were used for all PHB composites at each timepoint [6].

Unfortunately, the PHB with 40w% Mg samples were too brittle and porous so that some of the implants broke during the implantation process; other implants broke during bone healing and degradation of the Magnesium powder. Therefore, a region of interest could not be defined for all PHB with 40w% Mg implants and the new bone formation was not evaluated with Mimics<sup>®</sup>.

### 3.2.2 Push out tests

The bones were harvested after 1, 3, 6 and 9 months of implantation. Pictures are made an optical microscope for visual assessment of the implant and bone (see figure 3.13). In all samples, no degradation was visible and the surface stayed intact and

### 3 Results

---

smooth. Most of the samples showed good bone contact leading to different grades of bone ongrowth.

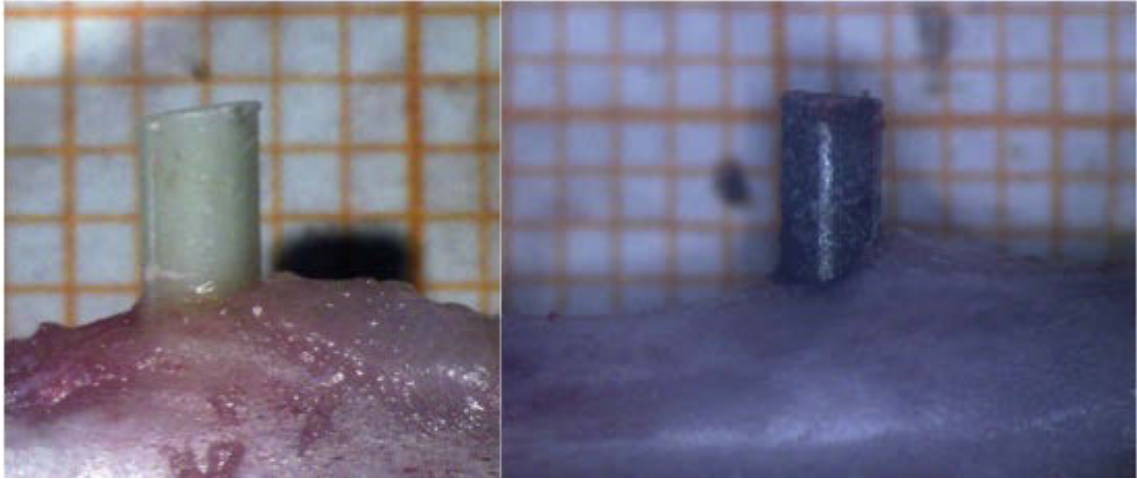


Figure 3.13: Explants after 1 month of implantation; left PHB with 30w% Herafill<sup>®</sup>, right PHB with 40w% Mg

The push out energy of the different PHB composites are shown in figure 3.14 and the shear strength results in figure 3.15. Unfortunately, the PHB with 40w% Mg samples were too brittle and broke during the healing process so only after 1 month push out tests could be performed which shows the lowest mechanical values for all materials. Also no push out tests were conducted of native PHB and PHB with 30w% Herafill<sup>®</sup> after 9 months.

After 1 month, energy absorption of PHB with 3w% Zircondioxide and 30w% Herafill<sup>®</sup> is significantly higher than within other composites, but the shear strength does not differ significantly. After 3 and 6 months energy absorption increases in some PHB types, but in all cases shear and energy absorption values stay still very low. Up to the sixth month, differences within the PHB composites are not significant [4].

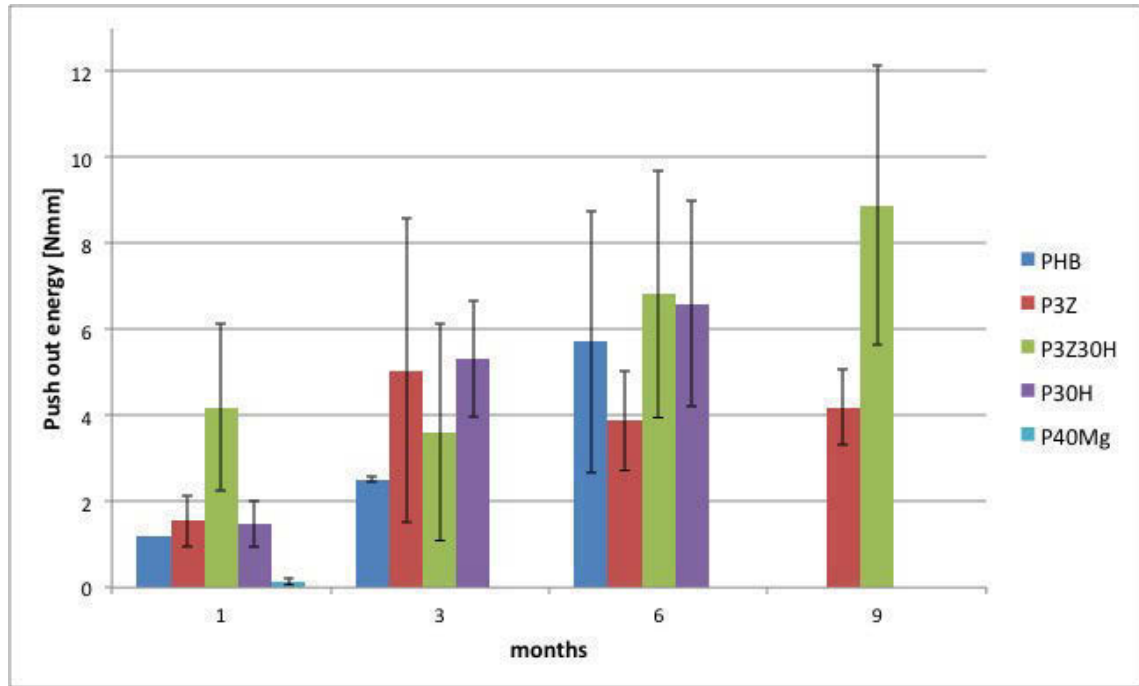


Figure 3.14: Push out results of PHB composites - the pin was displaced by pressing a cylindrical steel rod with constant velocity against it [4].

After 6 months, the composite only with Zircondioxide has the lowest push out energy and shear strength, the rest of the tested materials differ only slightly from each other. But after 9 months, shear strength and energy absorption of PHB with 3w% Zircondioxide and 30w% Herafill<sup>®</sup> is significantly higher than the values of PHB with 3w% Zircondioxide. High data scatter confirms large differences between the bones of the same implant group already observed in the optical evaluation.

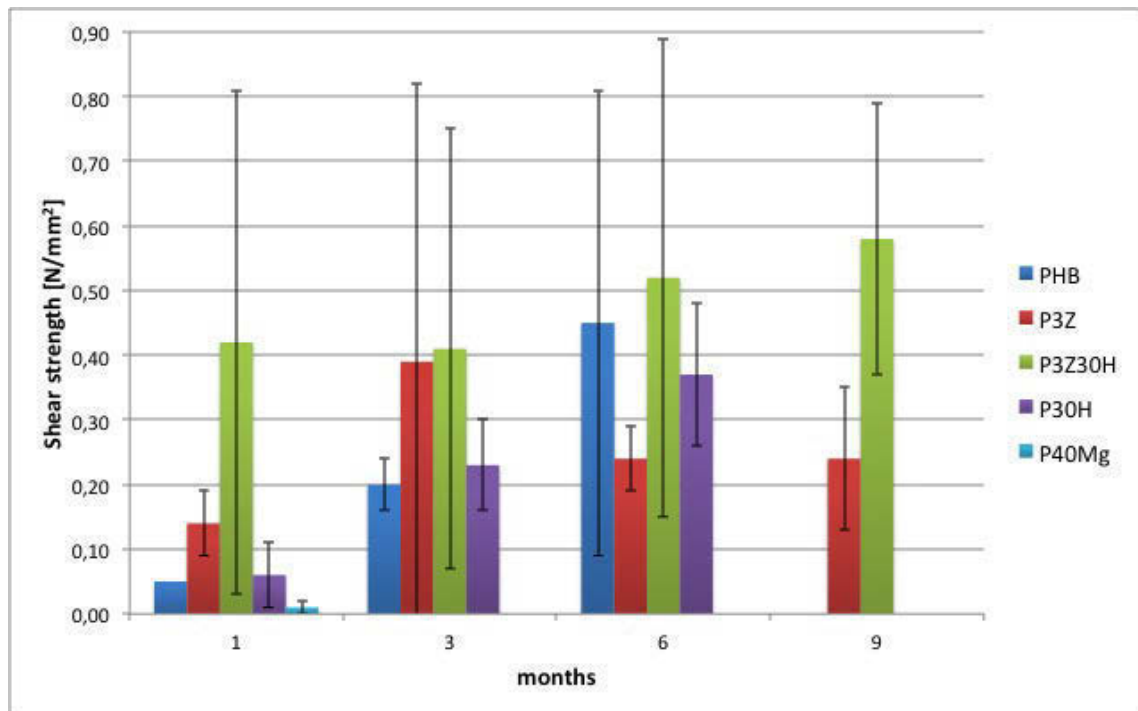


Figure 3.15: Share energy results of PHB composites - calculated by dividing the force maximum (point of failure) by the area of the implant bone interface [4].

### 3.2.3 Histological evaluation

The histological slices up to month 6 are performed (see examples in figure 3.16 to 3.18) and coloured with Levai-laczko staining. The cells stained in blue are mesenchymal cells from granulation tissue formed after trauma (drill) which differ in osteoblasts, secrete matrix and remain locked in the same. The cells stained in brown/grey are osteocytes, lamellae and osteons.

At the first month, no granulation tissue usually rich in macrophages, fibroblasts and capillaries were visible because of the advanced stage of bone repair. Also alamar

bone at braided fiber can be observed. Afterwards the osteoclasts (responsible for bone resorption) broke down the bone matrix with the formation of erosion channels. New osteoblasts provide the deposition of bone matrix in concentric lamellae, the channel of erosion shrink and perform a channel of Havers forming a new osteon.

In the first months, a cleft (in blue at higher resolution of figure 3.16 to 3.18) between implant and bone was created. These are undifferentiated and mesenchymal cells which differentiate in osteoblasts which again form the osteocytes. Over the time and the healing process, the bone fused with the implant. The black dots visible in the implant material are Zircon dioxide particles.

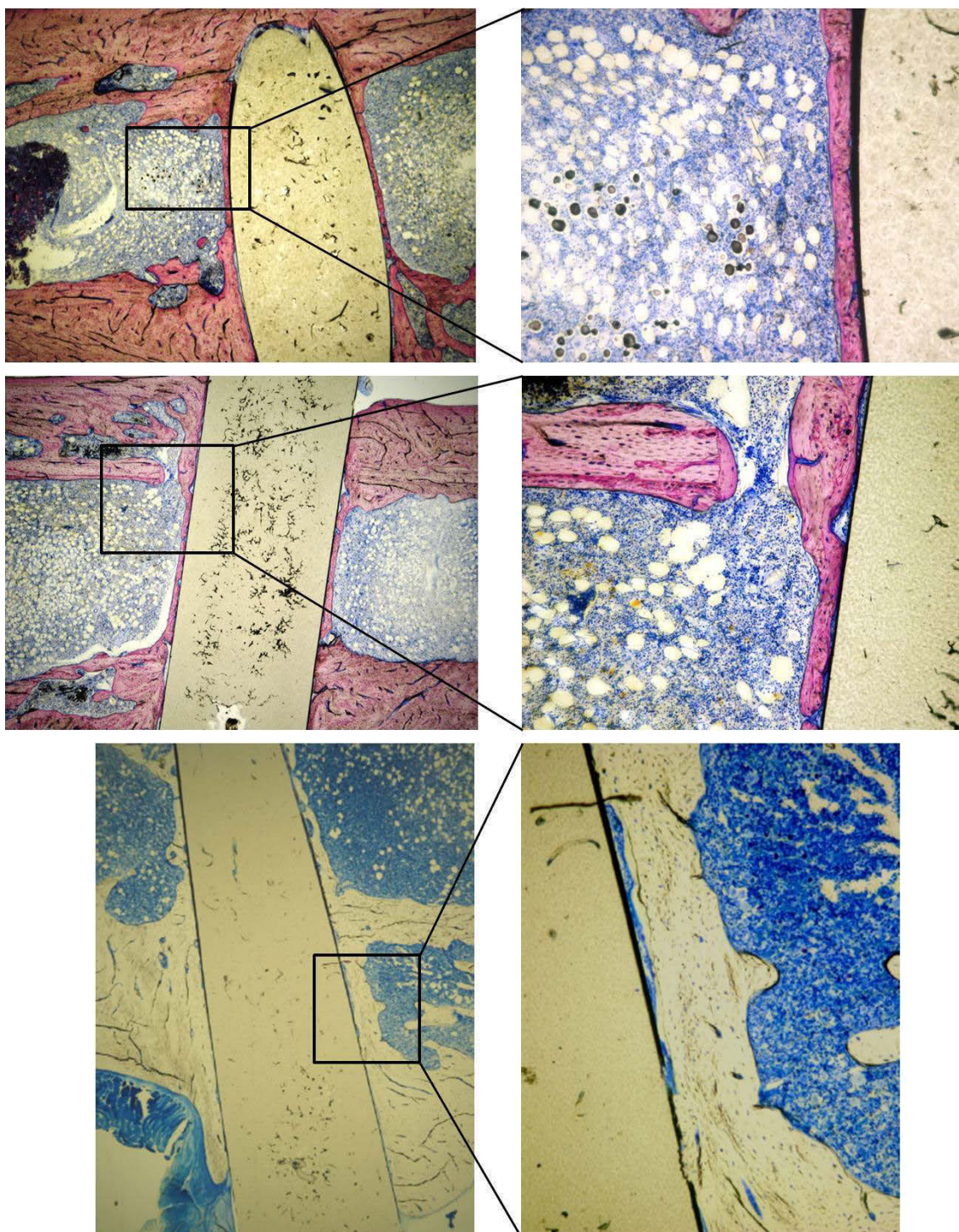


Figure 3.16: Histological slice of native PHB after 1, 3 and 6 months.

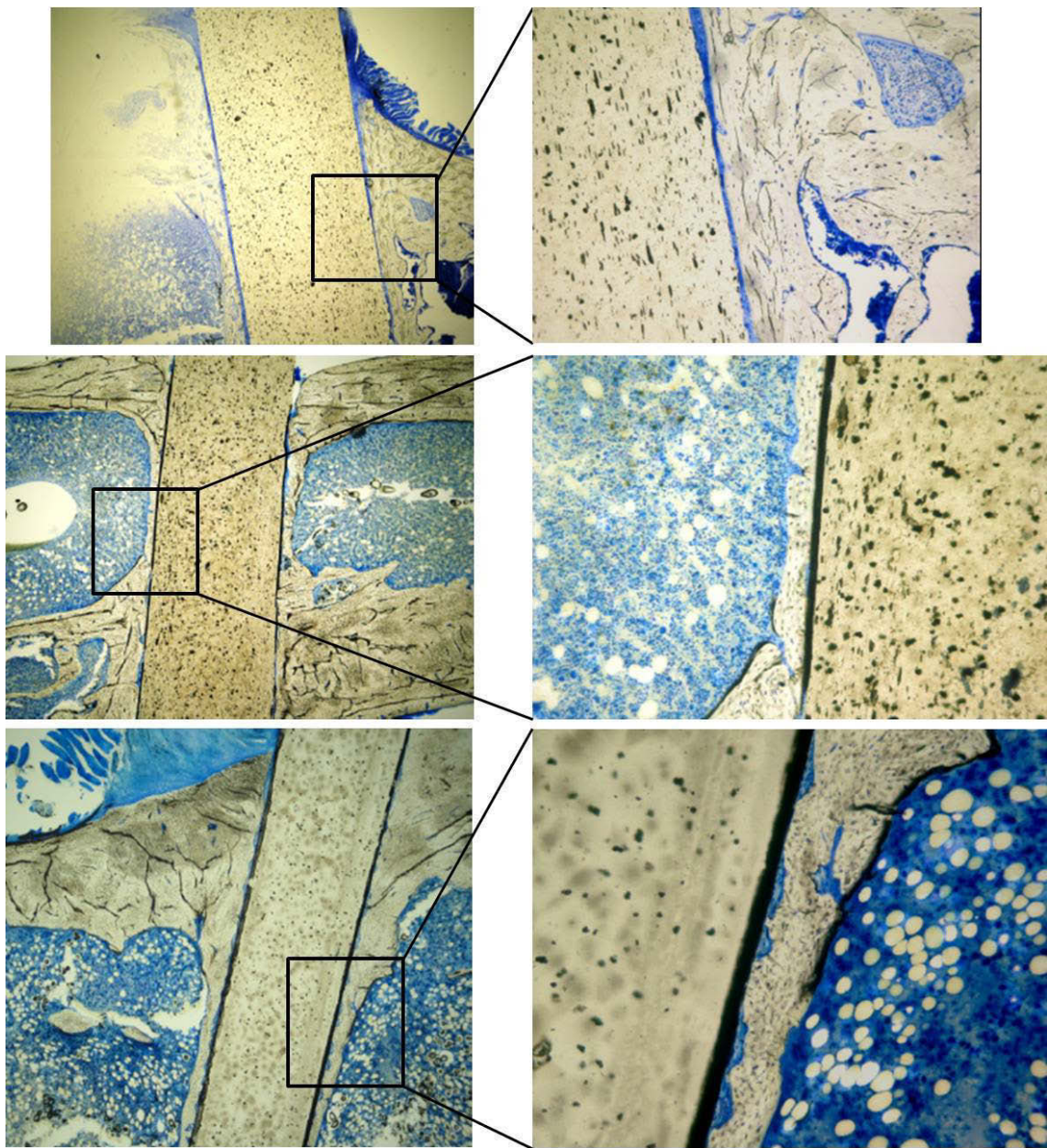


Figure 3.17: Histological slice of PHB with Zirconium dioxide after 1, 3 and 6 months.

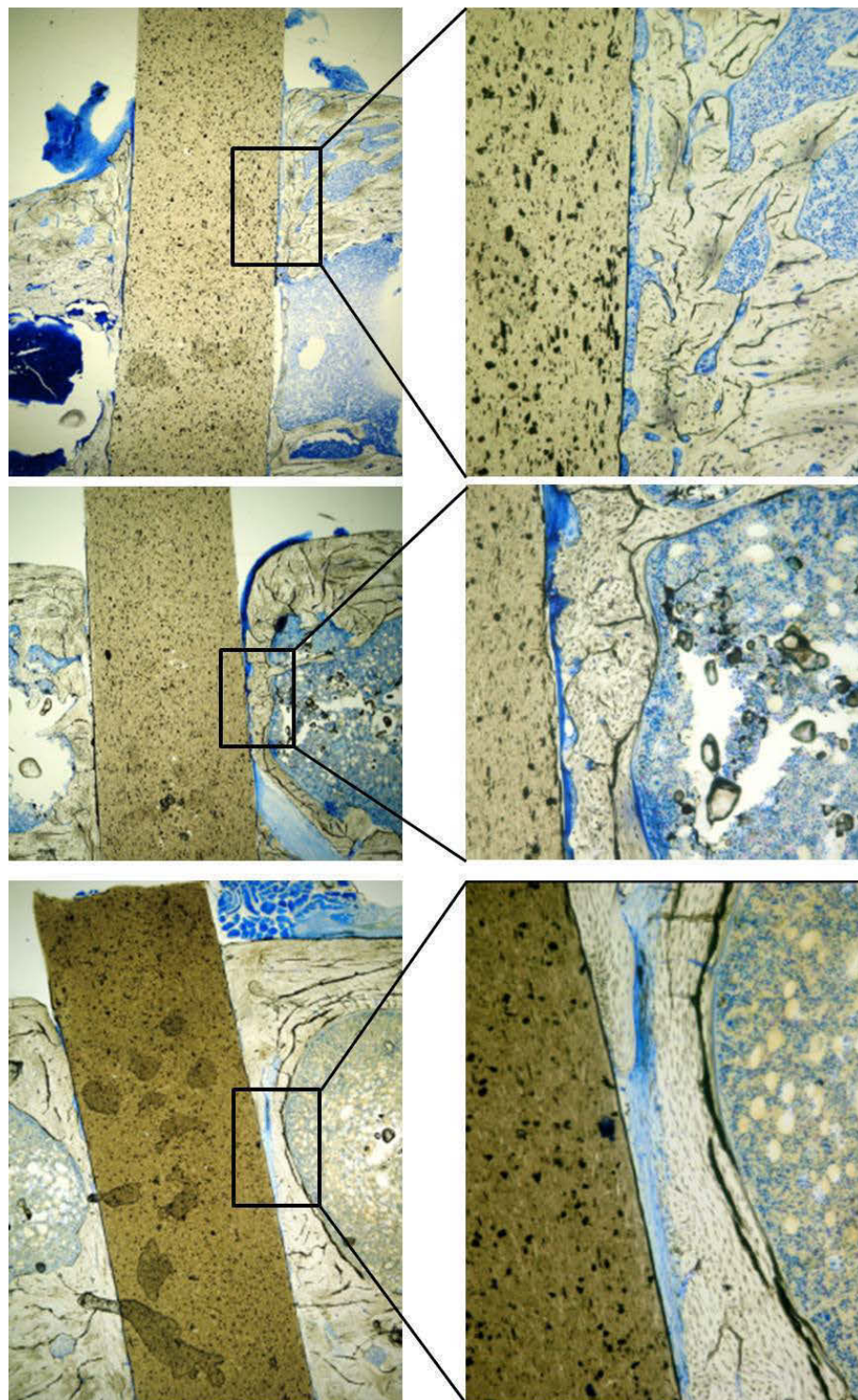


Figure 3.18: Histological slice of PHB with Zirconium dioxide and Herafill® after 1, 3 and 6 months.

### 3 Results

---

The histological analysis results of the mean bone adherence on the implant are documented in figure 3.19. Again, there was no changing of the mean bone adherence on the implant in the native PHB group (in blue) during 6 months. Also, a significant decrease ( $p = 0.024$ ) is obvious in the PHB with Zircondioxide group (in green) compared to the native PHB group (in blue). As seen in the  $\mu$ CT calculations, there is an increasing bone adherence in the group PHB with Zircondioxide and Herafill<sup>®</sup> (in purple) from month 1 to 6. Compared to PHB with Zircondioxide group (in green), a significant increase is visible in month 6.

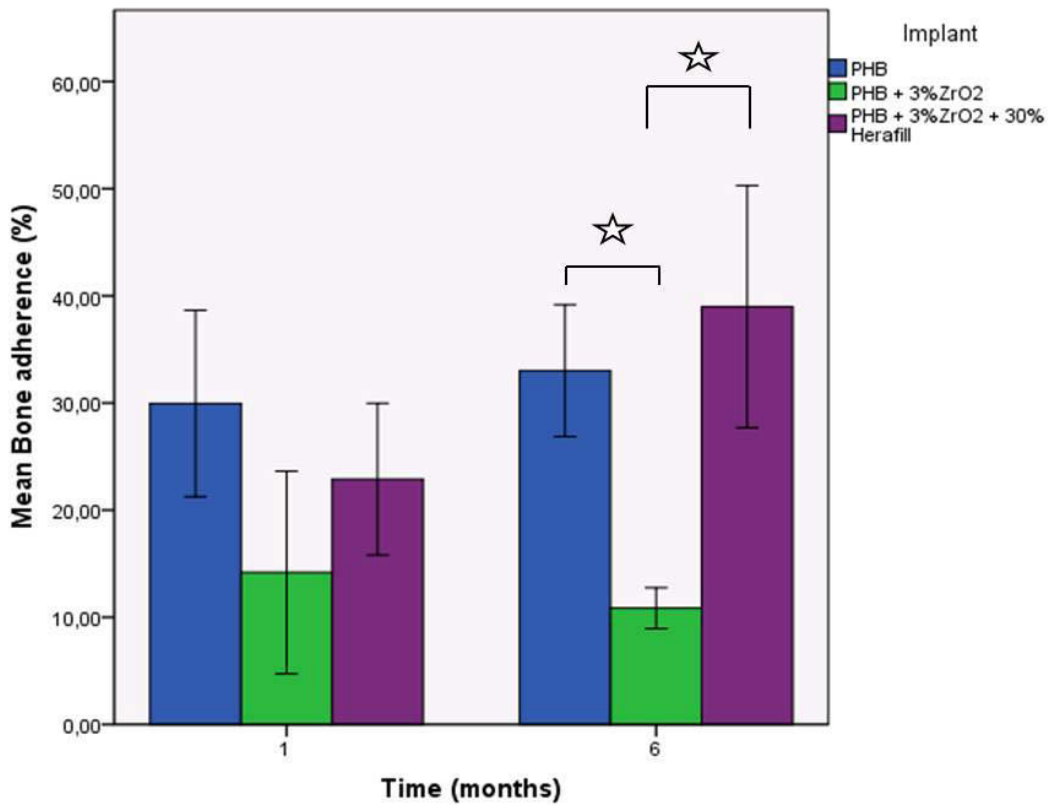


Figure 3.19: Results of mean bone adherence measurements on histological slices

### 3.3 Aim 3) Immunological response to bone injuries and implantation of a biodegradable polymer

PHB with 3w% ZrO<sub>2</sub> pins were successfully implanted in 12 femoral bones in 6 rats. Also, 12 femoral bones in 6 rats were drilled and used as Sham group. Additionally, 6 rats underwent no surgery and served as controls for blood examinations. No rat was lost during the study period and no bone got fractured.

#### 3.3.1 Phagocytic assay

##### **Group comparison:**

Before surgery, the phagocytic level of all 3 groups was similar and homogenous (see in figure 3.20). In the control group, the mean was about 61.1% (range: 37% - 73%, SD: 12.6), in the Sham group 51.15% (range: 47.8% - 54.3%, SD: 2.7) and in the experimental group B 63% (range: 47% - 92.1%, SD: 17.9). There were no significant differences between the groups. (C vs. S:  $p = 0.055$ ; C vs. B:  $p = 0.078$ ; S vs. B:  $p = 0.631$ ).

One week after surgery, the phagocytic activity of the cells decreased significantly in the Sham and experimental group. The lowest values were seen in the experimental group with implanted PHB. In the control group C, the mean was about 68.6% (range: 63.1% - 71.3%, SD: 10.77), in the Sham group S 56% (range: 40.2% - 54.0%, SD: 2.7) and in the experimental group B 41.13% (range: 26.8% - 62.8%, SD: 18.56). There were significant differences of group B and S compared to the control group C (C vs. S:  $p = 0.025$ ; C vs. B:  $p = 0.004$ ). The relation between

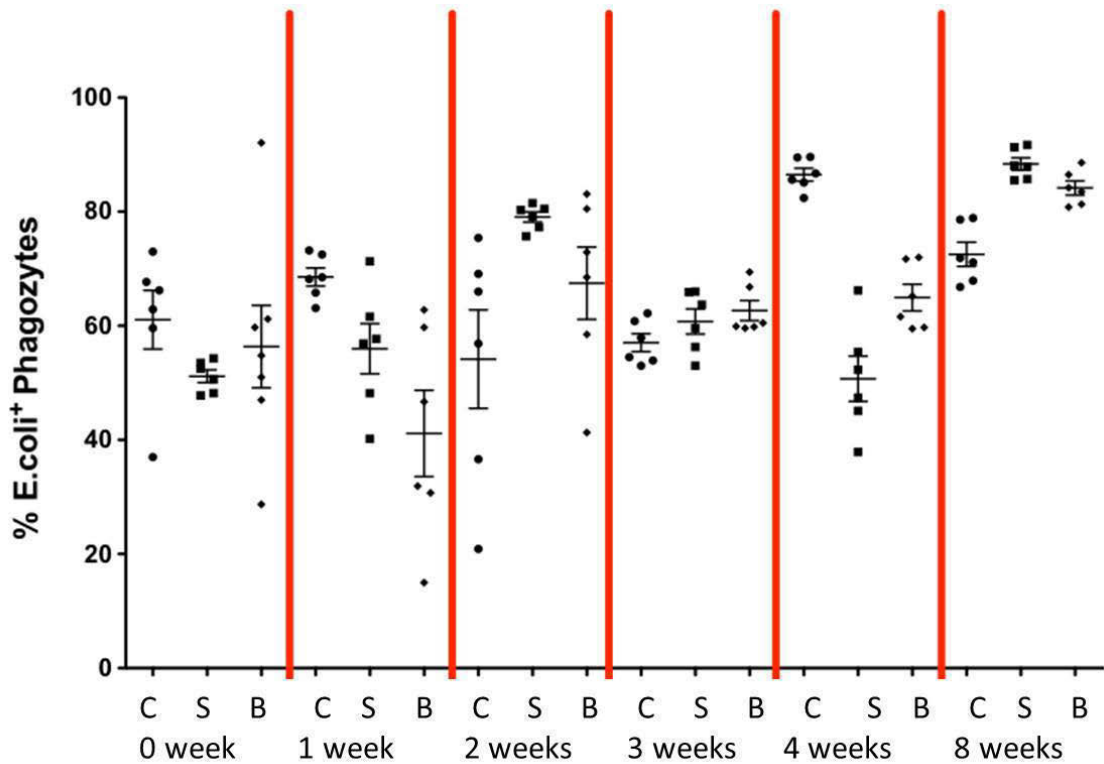


Figure 3.20: Phagocyte level during 8 weeks of observation in the control (C), Sham (S) and experimental group with PHB implant (B)

group B and S showed no significance ( $p = 0.20$ ).

After two weeks, the phagocytic activity increased significantly above the control group. The highest values were observed in group S, in the group with implanted bioresorbable PHB the difference was lower. In group C, the mean was about 60.8% (range: 36.6% - 75.4%, SD: 15.1), in the group S 79.1% (range: 75.7% - 81.5%, SD: 2.2) and in the group B 69.3% (range: 41.3% - 83.1%, SD: 16.7). In relation of group C and S, were again significant differences (C vs. S:  $p = 0.004$ ). But group C compared to group B or group S compared to group B showed no significance (C vs. B:  $p = 0.20$ , S vs. B:  $p = 0.229$ ).

Three weeks after surgery, in all groups the values were in the range before surgery. In the control group, the mean was about 57.5% (range: 53% - 62.2%, SD: 3.9), in the group S 60.8% (range: 53% - 66%, SD: 5.4) and in the group B 62.7% (range: 59.6% - 69.4%, SD: 4.3). There were no significant difference between the groups (C vs. S:  $p = 0.229$ ; C vs. B:  $p = 0.109$ ; S vs. B:  $p = 0.378$ ).

In the fourth week, again decreased levels in experimental and Sham group are observed. In the control group, the mean was about 86.5% (range: 82.4% - 89.6%, SD: 2.8), in the group S 50.7% (range: 37.9% - 66.2%, SD: 9.7) and in the group B 65% (range: 59.5% - 72%, SD: 5.7). There were significant differences of group B and S compared to the control group C (C vs. S:  $p = 0.004$ ; C vs. B:  $p = 0.004$ ). The relation between group B and S showed significant higher values in group B ( $p = 0.025$ ).

Compared to the control group, the phagocytic levels of both groups increased in week 8 after surgery. In the control group, the mean was about 72.5% (range: 66.8% - 78.9%, SD: 5.2), in group S 88.4% (range: 85.5% - 91.7%, SD: 2.7) and in group B 84.2% (range: 80.8% - 88.6%, SD: 3). There were no significant difference between the groups (C vs. S:  $p = 0.002$ ; C vs. B:  $p = 0.002$ , S vs. B:  $p = 0.055$ ).

#### **Group developing**

Group C:

During the first three weeks, the control group C had similar values (see in Table xx) and the Kruskal-Wallis test resulted in no significant differences in the group (week 0 to 1:  $p = 0.15$ ; week 1 to 2:  $p = 0.337$  and week 2 to 3:  $p = 0.631$ ). In the fourth week, the phagocytic activity increased significantly (week 3 to 4:  $p = 0.004$ ) on a maximum (mean: 86.48%). This can be explained due to the effect of habituation of the animals to the stressing blood sampling procedure. Also in week

8 are the phagocytic levels significantly higher than in the first three weeks (mean: 72.53%; week 4 to 8:  $p = 0.004$ ).

Group S:

In the Sham group S, the phagocytic activity increased on a maximum in the second postoperative week (79.1%). Compared to the start value (51.2%) and one week postoperative (56%), it was significantly higher (week 1 to 2:  $p = 0.004$ ).

Group B:

One week postoperative, a decrease of the phagocytic levels from 63% to 41.1% was observed in the experimental group B. But this difference was not statistically significant ( $p = 0.14$ ). During the second postoperative week, a significant increase to 69.3% was seen ( $p = 0.03$ ).

#### **3.3.2 Microfocus computed tomography *in vivo***

The Control group underwent no  $\mu$ CT examinations; they were used only as control for the phagocytic assay. In the Sham group, the drill hole was still present in the  $\mu$ CT scans one week after surgery (see in figure 3.21). In the 4th week after surgery, the healing process was finished and the drill hole was closed, but a remodelling of bone was observed. After 8 weeks of  $\mu$ CT observation, the drilled bone was totally healed, no further injuries were visible and the bone recovered completely. In the experimental group with the implant, a good bone adherence was observed during all weeks of examination (see figure 3.22). In the first week after surgery, the drill-hole close to the implant was still visible, but first new bone formation around the implant already started. After 4 weeks, this drill hole was closed, callus formation was present and new bone is formed on the implants' surface. After 8

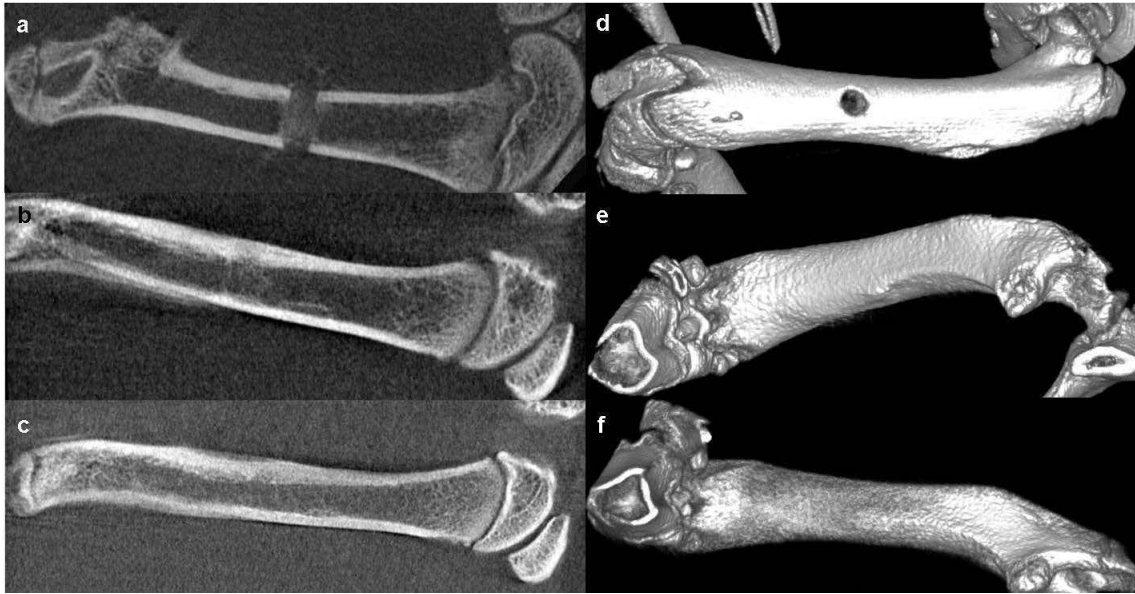


Figure 3.21: Sham group 1 week, 4 weeks and 8 weeks after surgery

weeks, additional new bone formation around the implant was present, the callus straightened, but no significant degradation of the material PHB was observed.



Figure 3.22: Experimental group 1 week, 4weeks and 8 weeks after surgery

## 4 Discussion

Within this thesis, polymeric composite materials based on PHB were evaluated for the use as orthopaedic load bearing implants. The influence of different additives on degradation behaviour, bone reaction, mechanical properties and bone-implant interface were investigated and the immunological response on the native PHB was tested. The transcortical implantation in a growing rat model and the longitudinal  $\mu$ CT scans offer a suitable method for polymeric materials to quantify degradation performance and new bone growth *in vivo* and *ex vivo*. The healing progress, mechanical interfacial strength, possible tissue irritation and bone remodelling can be systematically studied within the one animal.

### 4.1 Aim 1) In vivo degradation of novel bioresorbable composites in the femur of rats

Up to now, polymeric materials like PHB were not used for biodegradable fixation devices [27] because they show too long degradation times [64]. PHB is due to its low absorption of X-ray photons not visible in X-ray based imaging devices. To increase the contrast values within the microCT scans, Zirconiumdioxide was added to the native polymer. However, in vivo micro CT scans can be used to calculate

bone growth through examination of bone to tissue volume, but could not provide sufficient contrast between implant and new bone growth to evaluate the implant volume and surface [6].

Valid results of implant volume and surface were produced by high resolution ex vivo micro CT scanning of the bones. PHB and none of the composites P3Z and P3Z30H show any degradation after 9 months of implantation, in contrary, there is even an increase in volume. The swelling behaviour of PLGA in aqueous solution is reported in Dumitru et al [65] which could be also the reason for the volumeric increase of PHB observed in vivo. Compared to common polymers for medical application, the degradation time of PHB is closer to PLLA (more than 52 weeks) than to PLGA (4 - 52 weeks) or PGA (24 - 52 weeks) [33].

Herafill<sup>®</sup> is a trademarked bone graft substitute produced and distributed by Heraeus Medical GmbH Germany. It consists of a composite of calcium sulphate and calcium carbonate and is commonly used as a completely degradable substitute in bone defects [66, 67]. Preventing ingrowth of soft tissue, it should provide an osteoconductive matrix for the formation of new bone at the same time with its own gradual resorption. Its intended use was to degrade faster than PHB, enlarge the surface of the implants and therefore to accelerate degradation process of the polymer.

In all composite groups, no PHB degradation but also no adverse effects in bone tissue were visible. Only the Mg power added to PHB dissolved out of the implant and degraded within the bone. The PHB matrix was left unchanged within the bone, but due to its brittleness, the biomechanical forces of the bone healing process broke the implant.

## 4.2 Aim 2) Biocompatibility and osteoinductive properties of PHB bone implants

In this study, biocompatibility is defined as bone cell contact or even adhesion to the implant surface. The amount of new bone formation in the medullar cavity was seen as indicator for normal fracture healing and biocompatibility and not as adverse bone or tissue response. Suitable conditions for callus growth, cartilage and bone tissue are important requirements for a successful implant material [68].

During the whole study period, a continuous decrease of BV and BV/TV were observed around the implanted polymeric composites. Of all composite materials, the combination with Zirconiumdioxide and Herafill<sup>®</sup> seems to be most beneficial to bone accumulation [6]. In a case report, Herafill<sup>®</sup> beads G seemed to be a suitable osteoconductive material for bone reconstruction and showed promising results in treatment of chronic osteomyelitis [56].

The use of Zirconiumdioxide was suitable for the evaluation of the composites through microCT scans, because visibility and resolution were enhanced. But push out tests and the calculation of new bone volume in micro CT scans and histological slides suggest no further bone adherence or even decreasing amount of bone after one month of implantation. These results are in accordance with *in vivo* studies performed from Kohal et al [69]: Zirconia and titanium implants were examined to investigate the osteoblast and tissue response. The implants were integrated into the bone tissue, but the osseointegration of zirconia seemed to be slower and a lesser extent compared to titanium [69].

Further *in vitro* experiments with osteoblasts in culture showed that during the first days in culture, zirconia improved significantly cell proliferation, but does not

improve attachment and adhesion strength of the cells compared to titanium [70]. Nevertheless, Warashina et al. showed that ceramic particles like zircona and alumina had less induced inflammatory response and bone resorption compared to titanium and polyethylene [71]. Also a review by Manicone et al. proposed that zirconia has good biological and mechanical properties in clinical applications [72].

The addition of a resorbable bone graft substitute should enhance bone attachment and increase the degradation rate by reducing the total PHB content and by increasing the surface. However, these expectations have not been met.

The cleft visible within the first months in the histological slides support the push out results at the same time points. The bone contact seems to enhance around the implant during the study period. PHB and its composites exhibit no degradation at all, that's why their surface morphologies remain smooth and even during the whole implantation period. Also because of this, the shear strength and the energy absorption stay at very low levels [4].

The results of new bone growth and biocompatibility within this study conclude that the investigated PHB composites have to be classified as unsuitable as bone implants. Also improvement of the biomechanical properties (like strength, stiffness and fracture energy) of these composites is needed for using them as load bearing bone implant material [4].

### 4.3 Aim 3) Immunological response to bone injuries and implantation of a biodegradable polymer

In many comparative studies about common permanent implant materials like titan, nickel, cobalt, chrome and their alloys, the high immunoreactive potential is proved. Complications are mainly caused by corrosion of the material or particle and ion release out of the implant during friction and tissue contact. These waste products activate the monocytes and they produce increased amounts of pro-inflammatory cytokines like  $IL-1\beta$ ,  $TNF\alpha$ ,  $IL-6$ ,  $IL-8$ . The cytokines again decrease the activity of osteoblasts, but increase the activity of osteoclasts. Allergic and hypersensitivity reactions are the consequence, even osteolysis and implant loosening are possible [73, 74]. Therefore, bioresorbable implants like PHB seem to be a good alternative to common implant materials.

This study with 18 growing rats shows that the implanted material PHB has no additional influence on the immune system especially compared the phagocytic activity to simple bone injury with soft tissue trauma in the Sham group. The phagocytic levels of the control group remain more or less constant over the whole study period. Only in the 4th and 8th week a significant increase in the phagocytic ability is measured. A possible explanation can be that the animals have a kind of stressing effect during the blood sampling procedure in the beginning [75].

Instead of that, levels of the Sham group and the experimental group decreased but within these two groups, no significant differences can be observed. Only in the first postoperative week, the implanted material PHB induces further decrease of phagocytic activity compared to the Sham group. But in the following weeks, the levels

returned to the starting point. This effect suggests an immunosuppressive reaction to the implant that has been overcome during the study period. These decreased levels of group S and B in the first week are explained with the bone injuries and soft tissue trauma after surgery also described in the micro CT scans (figure 3.21 and 3.22). The increased phagocytic activity in the second week after surgery can be interpreted with a bone healing phase. As described of Menger et. al (2004), monocytes and macrophages secrete proinflammatory cytokines like  $\text{TNF-}\alpha$  and  $\text{IL-1}\beta$  at early stage after injury. These factors regulate additional cytokines production like IL-6 which is responsible for the neutrophil granulocyte proliferation in the bone marrow and enhance their activity. But also the following anti-inflammatory compensation mechanisms are triggered by IL-6. Mediators like prostaglandin (PG) E2, IL-10 and Transforming Growth Factor (TGF)  $\beta$  are proliferated and induce an immunosuppression [76]. Mountziaris et al. (2008) described a similar effect on the immune system during the bone healing process. Again in the first week, inflammatory reactions are present based on the proliferation of cytokines like IL-1, IL6 and  $\text{TNF-}\alpha$ . They also increase the amount of phagocytes and their activity [77].

In the third week, all levels are similar and again back at the starting point as a kind of resting phase after injury stabilization and stimulation of the healing process.

4 weeks after implantation, the drill hole is completely closed as observed in the  $\mu\text{CT}$  scans and bone remodelling to remove the now useless bone fragments is under progress. This remodelling process seems to decrease the phagocytic levels in the experimental group and further decrease them in the Sham group. Due to the inserted implant in the drill hole, there are less unnecessary bone fragments in the experimental group compared to the Sham group which can explain the different phagocytic levels.

Shishatskaya et al. published 2004 results of a rat model and showed that there

is no unwanted influence on the whole body after the use of pure PHB as sewing material [78]. Also Xiang-Hua Qu et al. reported only mild tissue reactions after subcutaneously implantation of PHB particles in rabbits [79] and Gogolewski et al. observed no adverse immunological reactions in the surrounding tissue after PHB pins implantation [24].

In the evaluation of the phagocytic activity, the differentiation between monocytes and granulocytes got difficult because of their similar size, granularity and the lack of working antibodies. That's why both cell populations are combined and only an overall sum is available.

## 5 Conclusion

Several aspects have to be addressed in the development of biodegradable implants for children:

Fracture healing is faster than in adults and therefore, biodegradable implants would be of substantial benefit in paediatric patients. Different steps regarding materials, biomechanics, the degradation in the bone and the bony answer to degradation have to be considered.

- PHB as an implant for children is in its native composition inappropriate due to its long degradation process seen in the  $\mu$ CT scans.
- Added Magnesium powder was degrading faster, but the remaining PHB showed no enhanced degradation process. The whole implant was getting too brittle and the push-out tests after 1 month showed the lowest forces of all tested PHB implants.
- Also the additives Zircon dioxide and Herafill<sup>®</sup> could not significantly accelerate the degradation process.

But, the high tolerance of tissue and bone to the implant in histological slices is in all PHB groups promising.

- The composites with Herafill<sup>®</sup> seem to be most attractive for bone cells.

- The composite with Zirconium dioxide show decreased bone formation around the implant.
- Even though Zirconium dioxide was added, the resolution between implant and surface was not high enough to get valid volume and surface values with  $\mu$ CT scans. But it was possible to compare bone reactions and new bone formations within the different PHB groups.
- The inflammatory study confirms that PHB as a bioresorbable implant do not provoke any significant further adverse effects compared to the Sham group, a good bone adherence and new bone formation can be observed in the  $\mu$ CT pictures.
- The loss of enzymatic activity in cortical bone and bone marrow surrounding the implant material could be a possible reason for the slow degradation of PHB.

Because of the low degradation rate at the one side and the good tissue and bone tolerance on the other side, other fields of application of PHB should be considered. Because of the good biocompatibility of PHB in bone and tissue, coatings should be mentioned and it is also an alternative to PLA which is used for sutures, coatings, stents, dialysis, scaffolds [80] and drug delivery devices.

# References

- [1] I. Marzi, ed., *Kindertraumatologie*. Berlin, Heidelberg: Springer Berlin Heidelberg, 2010.
- [2] A.-M. Weinberg and H. Tscherne, *Tscherne Unfallchirurgie: Unfallchirurgie im Kindesalter - Teil 1: Allgemeiner Teil, Kopf, Obere Extremität - Teil 2: Untere Extremität, Wirbelsäule, ... Besonderheiten des Kindlichen Skelettes*. Springer, 2006.
- [3] K. Angerpointner, *Phagocytotic activity after implantation of bioresorbable implants in rats*. PhD thesis, Medical University of Graz, 2012.
- [4] A. Celarek, T. Kraus, E. K. Tschegg, S. F. Fischerauer, S. Stanzl-Tschegg, P. J. Uggowitzer, and A. M. Weinberg, “PHB, crystalline and amorphous magnesium alloys: promising candidates for bioresorbable osteosynthesis implants?,” *Materials science & engineering. C, Materials for biological applications*, vol. 32, pp. 1503–10, Aug. 2012.
- [5] D. Eglin and M. Alini, “Degradable polymeric materials for osteosynthesis: Tutorial,” *European Cells and Materials*, vol. 16, pp. 80–91, 2008.
- [6] M. Meischel, J. Eichler, E. Martinelli, U. Karr, J. Weigel, G. Schmöller, E. Tschegg, S. Fischerauer, A. Weinberg, and S. Stanzl-Tschegg, “Adhesive

## References

---

- strength of bone-implant Interfaces and in-vivo degradation of PHB composites for load-bearing applications,” *Journal of the Mechanical Behavior of Biomedical Materials*, vol. 53, pp. 104–118, Aug. 2015.
- [7] N. Borse, J. Gilchrist, A. Dellinger, R. Rudd, M. Ballesteros, and D. Sleet, “Patterns of Unintentional Injuries among 0-19 Year Olds in the United States, 2000-2006,” p. 116, 2008.
- [8] E. Commission, *Injuries in the European Union: Summary of injury statistics for the years 2008-2010*. No. 4, 2013.
- [9] W. World Health Organization, “World report on child injury prevention,” *Geneva, Switzerland*, pp. 1–212, 2008.
- [10] E. Towner, T. Dowswell, G. Errington, M. Burkes, and J. Towner, *Injuries in Children aged 0–14 Years and Inequalities: A Report Prepared for the Health Development Agency*. 2005.
- [11] Susan P. Baker, Brian O’Neill, Marvin J. Ginsburg and G. Li, *The Injury Fact Book Second Edition*. 1992.
- [12] J. Matussek, *Kinderorthopädie und Kindertraumatologie*. Berlin, Heidelberg: Springer Berlin Heidelberg, 2013.
- [13] R. B. Salter, “Injuries of the epiphyseal plate.,” *Instructional course lectures*, vol. 41, pp. 351–9, Jan. 1992.
- [14] R. B. SALTER and W. R. HARRIS, “Injuries Involving the Epiphyseal Plate,” *J Bone Joint Surg Am*, vol. 45, pp. 587–622, Apr. 1963.
- [15] J. Matussek, *Kinderorthopädie und Kindertraumatologie*. Berlin, Heidelberg: Springer Berlin Heidelberg, 2013.

- [16] K. E. Wilkins, "Principles of fracture remodeling in children.," *Injury*, vol. 36 Suppl 1, pp. A3–11, Feb. 2005.
- [17] H. G. Dietz, P. Illing, P. P. Schmittenebecher, T. Slongo, and D. W. Sommerfeldt, eds., *Praxis der Kinder- und Jugendtraumatologie*. Berlin, Heidelberg: Springer Berlin Heidelberg, 2011.
- [18] D. R. Vinson and C. L. Hoehn, "Sedation-assisted Orthopedic Reduction in Emergency Medicine: The Safety and Success of a One Physician/One Nurse Model.," *The western journal of emergency medicine*, vol. 14, pp. 47–54, Feb. 2013.
- [19] Thomas P. Rüedi, Richard E. Buckley, Christopher G. Moran, *AO Principles of Fracture Management, Volume 1*. Thieme, 2007.
- [20] K. Pichler, S. Fischerauer, P. Ferlic, E. Martinelli, H.-P. Brezinsek, P. J. Uggowitzner, J. F. Löffler, and A.-M. Weinberg, "Immunological Response to Biodegradable Magnesium Implants," *JOM*, vol. 66, pp. 573–579, Feb. 2014.
- [21] R. Chung, B. K. Foster, and C. J. Xian, "Injury responses and repair mechanisms of the injured growth plate.," *Frontiers in bioscience (Scholar edition)*, vol. 3, pp. 117–25, Jan. 2011.
- [22] C. Castellani, R. a. Lindtner, P. Hausbrandt, E. Tschegg, S. E. Stanzl-Tschegg, G. Zanoni, S. Beck, and A. M. Weinberg, "Bone-implant interface strength and osseointegration: Biodegradable magnesium alloy versus standard titanium control," *Acta Biomaterialia*, vol. 7, no. 1, pp. 432–440, 2011.
- [23] M. Bohner, "Calcium orthophosphates in medicine: from ceramics to calcium phosphate cements.," *Injury*, vol. 31 Suppl 4, pp. 37–47, Dec. 2000.
- [24] S. Gogolewski, "Bioresorbable polymers in trauma and bone surgery.," *Injury*,

- vol. 31 Suppl 4, pp. 28–32, Dec. 2000.
- [25] M. Schinhammer, A. C. Hänzi, J. F. Löffler, and P. J. Uggowitzer, “Design strategy for biodegradable Fe-based alloys for medical applications,” *Acta Biomaterialia*, vol. 6, no. 5, pp. 1705–1713, 2010.
- [26] M. P. Staiger, A. M. Pietak, J. Huadmai, and G. Dias, “Magnesium and its alloys as orthopedic biomaterials: A review,” *Biomaterials*, vol. 27, pp. 1728–1734, 2006.
- [27] I. C. Bonzani, J. H. George, and M. M. Stevens, “Novel materials for bone and cartilage regeneration,” *Current Opinion in Chemical Biology*, vol. 10, pp. 568–575, 2006.
- [28] M. S. Taylor, A. U. Daniels, K. P. Andriano, and J. Heller, “Six bioabsorbable polymers: in vitro acute toxicity of accumulated degradation products.,” *Journal of applied biomaterials : an official journal of the Society for Biomaterials*, vol. 5, pp. 151–7, Jan. 1994.
- [29] A. Atlić, M. Koller, D. Scherzer, C. Kutschera, E. Grillo-Fernandes, P. Horvat, E. Chiellini, and G. BrauneGG, “Continuous production of poly([R]-3-hydroxybutyrate) by *Cupriavidus necator* in a multistage bioreactor cascade,” *Applied Microbiology and Biotechnology*, vol. 91, pp. 295–304, 2011.
- [30] R. Chandra, “Biodegradable polymers,” *Progress in Polymer Science*, vol. 23, pp. 1273–1335, Nov. 1998.
- [31] C. S. K. Reddy, R. Ghai, Rashmi, and V. C. Kalia, “Polyhydroxyalkanoates: An overview,” *Bioresource Technology*, vol. 87, pp. 137–146, 2003.
- [32] T. Saito and K. Tomita, “In vivo and in vitro degradation of poly ( 3-hydroxybutyrate ) in rat was,” *Science*, pp. 309–312.

- [33] D. Eglin and M. Alini, "Degradable polymeric materials for osteosynthesis: Tutorial," *European Cells and Materials*, vol. 16, pp. 80–91, 2008.
- [34] M. Koller, R. Bona, E. Chiellini, and G. Braunegg, "Extraction of short-chain-length poly-[(R)-hydroxyalkanoates] (scl-PHA) by the "anti-solvent" acetone under elevated temperature and pressure.," *Biotechnology letters*, vol. 35, pp. 1023–8, July 2013.
- [35] M. A. Eiteman and S. Ramalingam, "Microbial production of lactic acid.," *Biotechnology letters*, vol. 37, pp. 955–72, May 2015.
- [36] N. Jacquel, C.-W. Lo, Y.-H. Wei, H.-S. Wu, and S. S. Wang, "Isolation and purification of bacterial poly(3-hydroxyalkanoates)," *Biochemical Engineering Journal*, vol. 39, pp. 15–27, Apr. 2008.
- [37] D. F. Williams, "On the nature of biomaterials.," *Biomaterials*, vol. 30, pp. 5897–909, Oct. 2009.
- [38] D. F. Williams, "On the mechanisms of biocompatibility," *Biomaterials*, vol. 29, no. 20, pp. 2941–2953, 2008.
- [39] J. M. Anderson, A. Rodriguez, and D. T. Chang, "Foreign body reaction to biomaterials," *Seminars in Immunology*, vol. 20, no. 2, pp. 86–100, 2008.
- [40] R. van Lith, E. K. Gregory, J. Yang, M. R. Kibbe, and G. A. Ameer, "Engineering biodegradable polyester elastomers with antioxidant properties to attenuate oxidative stress in tissues.," *Biomaterials*, vol. 35, pp. 8113–22, Oct. 2014.
- [41] A. E. Engberg, P. H. Nilsson, S. Huang, K. Fromell, O. a. Hamad, T. E. Mollnes, J. P. Rosengren-Holmberg, K. Sandholm, Y. Teramura, I. a. Nicholls, B. Nilsson, and K. N. Ekdahl, "Prediction of inflammatory responses induced by biomaterials in contact with human blood using protein fingerprint from plasma,"

- Biomaterials*, vol. 36, pp. 55–65, 2015.
- [42] K. J. Schwenzer, “Protecting vulnerable subjects in clinical research: children, pregnant women, prisoners, and employees.,” *Respiratory care*, vol. 53, no. 10, pp. 1342–1349, 2008.
- [43] C. f. I. O. o. M. Sciences, “International ethical guidelines for biomedical research involving human subjects.,” *Bulletin of medical ethics*, pp. 17–23, Oct. 2002.
- [44] M. E. Broome, “Consent (assent) for research with pediatric patients.,” *Seminars in oncology nursing*, vol. 15, pp. 96–103, May 1999.
- [45] R. E. Kauffman, “Clinical Trials in Children,” *Paediatric Drugs*, vol. 2, pp. 411–418, Nov. 2000.
- [46] W. working Group, “ETHICAL CONSIDERATIONS FOR CLINICAL TRIALS PERFORMED IN CHILDREN,” *WHO*, no. October 2006, 2007.
- [47] R. Suuronen, P. Laine, T. Pohjonen, and C. Lindqvist, “Sagittal ramus osteotomies fixed with biodegradable screws: a preliminary report.,” *Journal of oral and maxillofacial surgery : official journal of the American Association of Oral and Maxillofacial Surgeons*, vol. 52, pp. 715–20; discussion 720–1, July 1994.
- [48] A. Tegnander, L. Engebretsen, K. Bergh, E. Eide, K. J. Holen, and O. J. Iversen, “Activation of the complement system and adverse effects of biodegradable pins of polylactic acid (Biofix) in osteochondritis dissecans.,” *Acta orthopaedica Scandinavica*, vol. 65, pp. 472–5, Aug. 1994.
- [49] J. Nagels, M. Stokdijk, and P. M. Rozing, “Stress shielding and bone resorption in shoulder arthroplasty.,” *Journal of shoulder and elbow surgery / American*

- Shoulder and Elbow Surgeons ... [et al.]*, vol. 12, pp. 35–9, Jan. 2003.
- [50] S. Holland, A. Jolly, M. Yasin, and B. Tighe, “Polymers for biodegradable medical devices,” *Biomaterials*, vol. 8, pp. 289–295, July 1987.
- [51] C. Castellani, R. a. Lindtner, P. Hausbrandt, E. Tschegg, S. E. Stanzl-Tschegg, G. Zanoni, S. Beck, and A. M. Weinberg, “Bone-implant interface strength and osseointegration: Biodegradable magnesium alloy versus standard titanium control,” *Acta Biomaterialia*, vol. 7, no. 1, pp. 432–440, 2011.
- [52] S. N. S. Anis, N. M. Iqbal, S. Kumar, and A. Al-Ashraf, “Increased recovery and improved purity of PHA from recombinant *Cupriavidus necator*,” *Bioengineered*, vol. 4, pp. 115–8, Jan.
- [53] A. Atlić, M. Koller, D. Scherzer, C. Kutschera, E. Grillo-Fernandes, P. Horvat, E. Chiellini, and G. Braunegg, “Continuous production of poly([R]-3-hydroxybutyrate) by *Cupriavidus necator* in a multistage bioreactor cascade,” *Applied Microbiology and Biotechnology*, vol. 91, pp. 295–304, 2011.
- [54] R. Gillani, B. Ercan, A. Qiao, and T. J. Webster, “Nanofunctionalized zirconia and barium sulfate particles as bone cement additives,” *International Journal of Nanomedicine*, vol. 5, pp. 1–11, 2010.
- [55] X. Gu, Y. Zheng, Y. Cheng, S. Zhong, and T. Xi, “In vitro corrosion and biocompatibility of binary magnesium alloys,” *Biomaterials*, vol. 30, no. 4, pp. 484–498, 2009.
- [56] M. Franceschini, A. Di Matteo, H. Bösebeck, H. Büchner, and S. Vogt, “Treatment of a chronic recurrent fistulized tibial osteomyelitis: Administration of a novel antibiotic-loaded bone substitute combined with a pedicular muscle flap sealing,” *European Journal of Orthopaedic Surgery and Traumatology*, vol. 22,

- pp. 245–249, 2012.
- [57] T. Kraus, S. F. Fischerauer, A. C. Hänzi, P. J. Uggowitzer, J. F. Löffler, and A. M. Weinberg, “Magnesium alloys for temporary implants in osteosynthesis: In vivo studies of their degradation and interaction with bone,” *Acta Biomaterialia*, vol. 8, pp. 1230–1238, 2012.
- [58] W. Hirt, T. Nebe, and C. Birr, “[Phagotest and Bursttest (Phagoburst), test kits for study of phagocyte functions].,” *Wiener klinische Wochenschrift*, vol. 106, pp. 250–2, Jan. 1994.
- [59] J. H. Kinney, N. E. Lane, and D. L. Haupt, “In vivo, three-dimensional microscopy of trabecular bone.,” *Journal of bone and mineral research : the official journal of the American Society for Bone and Mineral Research*, vol. 10, pp. 264–70, Feb. 1995.
- [60] L. A. Feldkamp, S. A. Goldstein, A. M. Parfitt, G. Jesion, and M. Kleerekoper, “The direct examination of three-dimensional bone architecture in vitro by computed tomography.,” *Journal of bone and mineral research : the official journal of the American Society for Bone and Mineral Research*, vol. 4, pp. 3–11, Feb. 1989.
- [61] J. Weigel, *Osseointegration von resorbierbaren Implantaten aus Poly(38hydroxy)butyrat: Untersuchung am Rattenmodell durch in vivo Mikro Computer Tomographie*. PhD thesis, Medical University of Graz, 2012.
- [62] G. Schmoeller, *In vivo and ex vivo  $\mu$ CT evaluations of biodegradable poly(3-hydroxybutyrate) implants in a rat model*. PhD thesis, Medical University of Graz, 2014.
- [63] R. Nalçacı, F. Oztürk, and O. Sökücü, “A comparison of two-dimensional radio-

- graphy and three-dimensional computed tomography in angular cephalometric measurements.,” *Dento maxillo facial radiology*, vol. 39, pp. 100–6, Feb. 2010.
- [64] S. Li, “Hydrolytic degradation characteristics of aliphatic polyesters derived from lactic and glycolic acids,” *Journal of Biomedical Materials Research*, vol. 48, pp. 342–353, 1999.
- [65] A. C. Dumitru, F. M. Espinosa, R. Garcia, G. Foschi, S. Tortorella, F. Valle, M. Dallavalle, F. Zerbetto, and F. Biscarini, “In situ nanomechanical characterization of the early stages of swelling and degradation of a biodegradable polymer.,” *Nanoscale*, vol. 7, pp. 5403–10, Mar. 2015.
- [66] D. C. Coraça-Huber, A. Wurm, M. Fille, J. Hausdorfer, M. Nogler, S. Vogt, and K.-D. Kühn, “Antibiotic-loaded calcium carbonate/calcium sulfate granules as co-adjuvant for bone grafting,” *Journal of Materials Science: Materials in Medicine*, vol. 26, p. 19, Jan. 2015.
- [67] D. Coraça-Huber, J. Hausdorfer, M. Fille, M. Nogler, and K.-D. Kühn, “Calcium carbonate powder containing gentamicin for mixing with bone grafts.,” *Orthopedics*, vol. 37, pp. e669–72, Aug. 2014.
- [68] M. Papakyriacou, “Effects of surface treatments on high cycle corrosion fatigue of metallic implant materials,” *International Journal of Fatigue*, vol. 22, pp. 873–886, 2000.
- [69] R. J. Kohal, M. Bächle, W. Att, S. Chaar, B. Altmann, A. Renz, and F. Butz, “Osteoblast and bone tissue response to surface modified zirconia and titanium implant materials.,” *Dental materials : official publication of the Academy of Dental Materials*, vol. 29, pp. 763–76, July 2013.
- [70] R. Depprich, M. Ommerborn, H. Zipprich, C. Naujoks, J. Handschel, H.-P.

- Wiesmann, N. R. Kübler, and U. Meyer, "Behavior of osteoblastic cells cultured on titanium and structured zirconia surfaces.," *Head & face medicine*, vol. 4, p. 29, Jan. 2008.
- [71] H. Warashina, S. Sakano, S. Kitamura, K. I. Yamauchi, J. Yamaguchi, N. Ishiguro, and Y. Hasegawa, "Biological reaction to alumina, zirconia, titanium and polyethylene particles implanted onto murine calvaria.," *Biomaterials*, vol. 24, pp. 3655–61, Sept. 2003.
- [72] P. F. Manicone, P. Rossi Iommetti, and L. Raffaelli, "An overview of zirconia ceramics: basic properties and clinical applications.," *Journal of dentistry*, vol. 35, pp. 819–26, Nov. 2007.
- [73] N. J. Hallab and J. J. Jacobs, "Biologic effects of implant debris.," *Bulletin of the NYU hospital for joint diseases*, vol. 67, pp. 182–8, Jan. 2009.
- [74] S. B. Goodman, "Wear particles, periprosthetic osteolysis and the immune system.," *Biomaterials*, vol. 28, pp. 5044–8, Dec. 2007.
- [75] M. D. Menger and B. Vollmar, "Surgical trauma: hyperinflammation versus immunosuppression?," *Langenbeck's archives of surgery / Deutsche Gesellschaft für Chirurgie*, vol. 389, pp. 475–84, Nov. 2004.
- [76] P. M. Mountziaris and A. G. Mikos, "Modulation of the inflammatory response for enhanced bone tissue regeneration.," *Tissue engineering. Part B, Reviews*, vol. 14, pp. 179–86, June 2008.
- [77] E. I. Shishatskaya, T. G. Volova, A. P. Puzyr, O. A. Mogilnaya, and S. N. Efremov, "Tissue response to the implantation of biodegradable polyhydroxyalkanoate sutures.," *Journal of materials science. Materials in medicine*, vol. 15, pp. 719–28, June 2004.

## References

---

- [78] X.-H. Qu, Q. Wu, K.-Y. Zhang, and G. Q. Chen, “In vivo studies of poly(3-hydroxybutyrate-co-3-hydroxyhexanoate) based polymers: biodegradation and tissue reactions.,” *Biomaterials*, vol. 27, pp. 3540–8, July 2006.
- [79] M. Nakagawara, K. Takeshige, J. Takamatsu, S. Takahashi, J. Yoshitake, and S. Minakami, “Inhibition of superoxide production and Ca<sup>2+</sup> mobilization in human neutrophils by halothane, enflurane, and isoflurane.,” *Anesthesiology*, vol. 64, pp. 4–12, Jan. 1986.
- [80] H. Schliephake, M. Vucak, J. Boven, S. Backhaus, T. Annen, and M. Epple, “Solvent free production of porous PDLA/calcium carbonate composite scaffolds improves the release of bone growth factors.,” *Oral and maxillofacial surgery*, vol. 19, pp. 133–41, June 2015.

# Appendices